AN INVESTIGATION, COMPARISON, AND DEVELOPMENT OF INDIVIDUAL TREE COMPETITION MODELS

by

Thomas G. Matney

Dissertation submitted to the Graduate Faculty of the
Virginia Polytechnic Institute and State University
in partial fulfillment of the requirements for the degree of
DOCTOR OF PHILOSOPHY
in
Forestry and Forest Products

APPROVED:

H. E. Burkhart, Chairman

R. E. Adams

J. C. Arnold

R. B. Vasey

M. R. Reynolds

June, 1976

Blacksburg, Virginia

ACKNOWLEDGMENTS

My gratitude is extended to R. E. Adams, J. C. Arnold, R. B. Vasey, M. R. Reynolds, and Richard F. Daniels for their invaluable help and constructive criticism in the preparation of this manuscript. I also wish to thank Westvaco for their courtesy in allowing me to use their property for data collecting; Mrs. Beth Burch for her expert typing; and my wife, Roberta, without whose loyalty and patience this dissertation would not have been possible. Special thanks is extended to the chairman of my committee, Dr. H. E. Burkhart whose aid in the preparation of the manuscript was a tremendous help.

The work herein reported was funded in part by a U.S. Department of Agriculture sponsored program entitled "The Expanded Southern Pine Beetle Research and Applications Program." The findings, opinions, and recommendations expressed herein are those of the author and not necessarily those of the U.S. Department of Agriculture (Grant number CSRS 516-15-58).

TABLE OF CONTENTS

LIST OF TABLES

LIST OF FIGURES

INTRODUCTION AND JUSTIFICATION

A typical silvicultural experimental technique consists of subjecting plots or stands to various treatments such as thinning or fertilization and observing one or more responses of interest. Inferences about the direction of the responses are made by comparisons with control plots. To extract reasonable inferences from this type of experimentation, it is necessary that large numbers of treatment combinations be applied to experimental units (stands or plots) of similar structure (homogeneous). Usually the location of a sufficient number of experimental units is virtually impossible, even if the cost of applying the necessary treatment combinations is feasible and justified. Dawkins (1960) and Johnson and Waters (1962) all stress the difficulties of defining thinning regimes. Johnson and Waters (1962), Wicht (1936) and Vezina (1962) have all mentioned the need for research with the objective of finding a measure of stand density that is suitable for statistical analysis. In light of these problems, the silviculturist often relies on the assignment of a few treatments to a small number of experimental units of very dissimilar stand structure, and draws what inferences he can. Thus, the necessity of diverging from plot-type experiments in silvicultural research is apparent, but what are the alternatives?

Since 1964, foresters have come to realize that the problems of plot experiments could be avoided by considering the response of

individual trees to treatment. Smith (1959) outlines the advantages of individual tree measurements in thinning experiments. Originally suggested in 1939 by Osborne, this technique, however, requires that one predict the response of each tree with and without treatment. One approach to the problem of predicting individual tree response is to quantify the competitive stress on each tree as a function of the size and spatial arrangement of other trees influencing it. The computed numerical value is called a competition index or competition quotient and it is an attempt to quantify competition, which may qualitatively be defined as the stress exerted on an individual tree by other trees for the limited resources necessary for the tree's growth processes. A difficulty with this approach has been in finding a suitable mathematical rule which maps sets of tree characteristics and spatial arrangements into a numerical index that predicts the desired response with adequate precision. In fact, even determining what trees in a stand are competing with each other has been a problem.

If an adequate competition model (mathematical rule) can be found then it can be applied as an invaluable aid in silvicultural research. Not only can it be used to gauge the response of individual trees to silvicultural treatments, but also as an essential component of stand simulation models.

This study dealt with the problem of finding a mathematical function which maps individual tree characteristics and spatial arrangement into real values which are functionally related to individual tree diameter increments. The investigative procedure consisted of:

1. Expanding a concept of recently advanced competition models (the mathematical rule) which shows great promise.

2. Comparing the diameter prediction efficiency of proposed and selected previous models on two data sets obtained from two old-field loblolly pine plantations.

BACKGROUND

Since 1964, numerous competition models have been proposed and tested under a variety of conditions. Also, in recent years, several articles have been published on the space occupancy of trees above and below ground in relation to various tree characteristics. These articles on space occupancy tend to lend credence to some of the competition models developed, especially the zone of influence models; thus, these papers will be cited where appropriate in the following literature review of previous individual tree competition models.

Basically, to date, three distinct concepts have been advanced in the development of individual tree competition models. These are:

1. Area potentially available
2. Circular zones of influence
3. Point density.

The above concepts will be used to divide the literature review into topics of discussion. Approaches to predicting diameter and basal area increments of interest but not qualifying as competition models are included in a fourth topic, other techniques.

The Area Potentially Available Concept

Brown (1965) assumed that in a stand, each tree has one-half the distance between itself and its nearest neighbor available for occupancy. By plotting the trees of a stand and drawing in perpendicular

bisectors of lines drawn between trees, a series of closed polygons result with a tree enclosed in each. Brown proposed that the area of each tree's enclosing polygon was a measure of the tree's potential growing space (APA) and 1/APA was a measure of individual tree competition. The measure (1/APA) showed a weak trend with basal area increments of 148 Pinus patula trees. The model, however, probably has limited application since it only considers the spatial arrangements of trees within a stand and does not include any provision for consistently evaluating each tree's competitive status in relation to the size of its neighbors. In other words, a large, fast-growing tree could have several trees in close proximity and thus be assigned a small APA and, as a result, be considered in a poor competitive position when, in fact, it may not be.

Moore, Budelsky and Schlesinger (1973) extended Brown's APA model. Instead of assuming a tree occupies half the distance (L) between itself and a neighbor, a subject tree is chosen and on the line connecting it with its j^{th} competitor, a perpendicular intersecting line is constructed at a distance of $\frac{D^2}{D^2+D_j^2}$ from the subject tree, where D = d.b.h. of the subject tree and D_j = d.b.h. of the subject tree's j^{th} competitor. This procedure, like Brown's, yields APA's which are mutually exclusive to those of other trees, but which are dependent on the relative sizes of trees as well as their spatial arrangement. Field trials of the extended APA model accounted for, respectively, 69, 61, and 72 percent of the variation of ten-year

basal area increments of black oak (Quercus velutina L.), white oak (Q. alba L.) and yellow poplar (Liriodendron tulipifera L.)

The Circular Zone of Influence Concept

The zone of influence models are all based upon the long established concept that when a tree is left free to grow, its growth limits (lateral root spread) approximate a circle (Aaltonen, 1926; Rogers, 1935). This zone of influence may be defined as the total area over which a tree may, at present, obtain or compete for site factors. Staebler (1951) was the first to develop the above concept into an individual tree competition model. He proposed that a tree's zone of influence radius (R) was a linear function of the tree's d.b.h. That is, $R = A + B$ (d.b.h.), where R = the radius of influence and A and B are constants to be determined. Smith (1964) reported that lateral root spread was closely related to the crown width of Douglas-fir (Pseudotsuga menziesii mirb.), lodgepole pine (Pinus contorta Dougl.) and other British Columbia tree species. Other variables found to be highly correlated to lateral root spread but less so than crown width were d.b.h., total age, and height. This probably holds true for many species and can be assumed to have wide applicability. That crown width is highly correlated with various measures of tree size for a number of species is well documented (Ilvessale, 1950 ; Minor, 1951; Wilson, 1955; Krajicek and Brinkman, 1957; Gruschow and Evans, 1959; Warrack, 1959; Vezina, 1962; and others). Smith and Dubow (1960) report on crown width to d.b.h. ratio and the crown width to total height ratio.

Staebler (1951) further suggested that in a stand, two trees are in competitive stress with each other if their circles of influence overlapped and this competition was measured by the linear overlap between the two trees' competition radii. He concluded that the total competitive stress exerted on an individual tree (subject tree) by its competitors was given by

$$CI = \sum_{k=1}^{n} d_k$$

where CI = Staebler's competition index

d_k = the linear overlap between the subject tree and its k^{th} competitor

and n = number of competitors

Staebler attempted to predict 12-year diameter increments of 32 Douglas-fir trees by choosing the constants A and B such that when the diameter increment was related to a polynomial regression equation in CI, the percent of variation accounted for was maximized. His results were, however, inconclusive.

Gerrard (1969) extended Staebler's results by using areas of overlaps rather than linear overlaps on the basis that it provided a more direct measure of competition. This hypothesis resulted in an index given by

$$CQ = \frac{1}{A} \sum_{k=1}^{n} a_k$$

where CQ = Gerrard's competition quotient

A = area of the subject tree's competition circle

a_k = area of overlap of the subject tree's competition with that of the k^{th} competitor

and n = number of competitors.

For the reader's reference, the following algorithm can be used to find the area of overlap (AOVL) between two circles of radii R1 and R2 with the respective rectangular coordinates of each circle's center being given by (X_1, Y_1) and (X_2, Y_2).

1. Compute $D = [(X_2 - X_1)^2 + (Y_2 - Y_1)^2]^{1/2}$, (the distance between the circle centers)
2. If $R1 + R2 \leq D$ set AOVL = 0 (i.e., no overlap occurred)
3. If $R1 \geq R2$, go to 5 and continue
4. If $R1 < R2$, do steps A to C to create the condition $R1 \geq R2$.
   A. R = R2, where R is a dummy variable
   B. R2 = R1
   C. R1 = R
5. Calculate the X coordinate of circle intersection as $Z = \frac{(R_1^2 - R_2^2 + D^2)}{1(2D)}$ assuming the center of the circle of radius R1 is translated to (0, 0) and the center of the circle of radius R2 is translated to (0, 0)
6. If $D \geq R1$, set $AOVL = R_1^2 \cos^{-1}(Z/R_1) + R2^2 \cos^{-1}[(-D-Z)/R2] - D[R1^2 - X^2)]^{1/2}$ (case 1 in Figure 1)
7. If $D < R1$ and $(R1 - D) < R2$, set $AOVL = \pi R2^2 + R1^2 \cos^{-1}(Z/R2) - Z[R1^2 - X^2]^{1/2} - R2^2 \cos^{-1}[(Z-D)/R2] + R2^2 \text{Sin}[2 \cos^{-1}\{Z-d/R2\}]/2$. (case 2 in Figure 1)
8. If not 6 or 7 set $AOVL = \pi R2^2$. (case 3 in Figure 1)

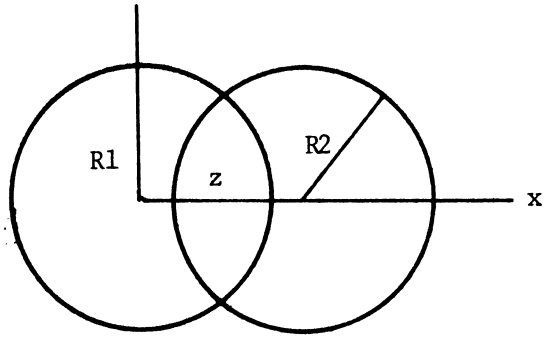

Case 1. First circle does not overlap the second circle's center

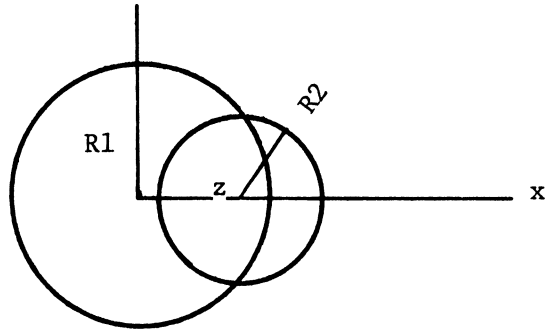

Case 2. First circle overlaps the second circle's center but does not completely overlap the second

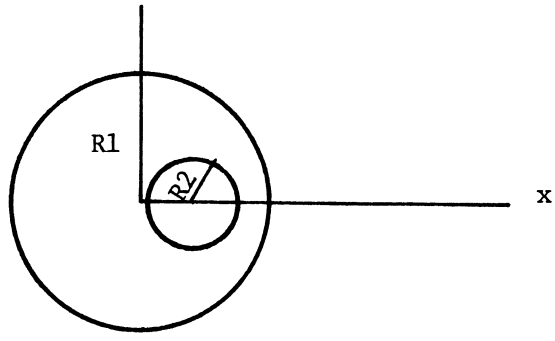

Case 3. First circle completely overlaps the second circle

Figure 1. Possible cases of overlapping circles when the first circle's radius (R1) is greater than the second circle's radius (R2).

See Gerrard (1969) for details of the formulae derivation.

In mixed hardwood stands comprised largely of red oak (Quercus rubra L.) and white oak (Q. alba L.) Gerrard compared his competition quotient with Newnham's (1964) competition index and Spurr's (1962) point density for their relative effectiveness in predicting 10-year basal area increments. Gerrard asserted that once the effect of d.b.h. had been removed in all regression equations, the contribution of his competition quotient was significant and it proved to be a stronger predictor variable than either Newnham's competition index or Spurr's point density. Newnham's index is defined as $1/2\pi$ times the sum of angles (in radians) subtended at the subject tree circle center by the common chords of overlapping circles (Newnham, 1964)(Figure 2). Spurr's point density concept is discussed later.

Bella (1972) further extended Gerrard's competition quotient by asserting that the relative contribution of each area of overlap depended on the relative sizes of the competitor. On this premise, he proposed the competition index

$$CIO = \frac{1}{A} \sum_{j=1}^{n} \left(\frac{D_j}{D}\right)^{EX} a_j$$

where CIO = Bella's competitive influence zone overlap

A = area of subject tree's competition circle

D_j = d.b.h. of j^{th} competitor

D = d.b.h. of subject tree

a_j = area of overlap between the subject tree and its j^{th} competitor

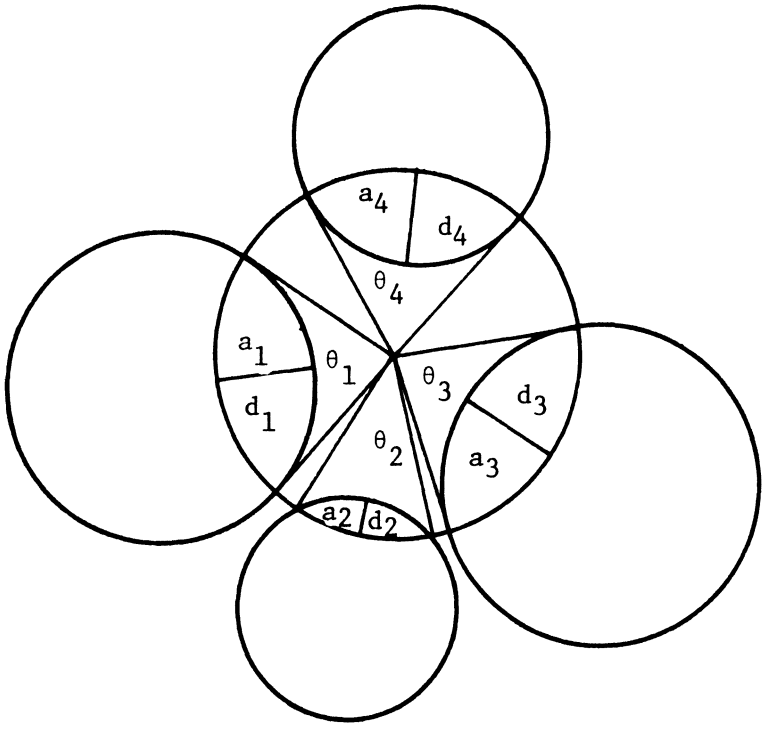

Staebler's

$$DI = \sum_{k=1}^{n} d_k$$

Newnham's $CI = \frac{1}{2} \sum_{k=1}^{n} \theta_k$

Gerrard's $CA = \frac{1}{A} \sum_{k=1}^{n} a_k$

where d_k = linear overlap between the subject tree and its k^{th} competitor.

θ_k = angle subtend from the subject tree's center to the common chord between subject tree and its k^{th} competitor

a_k = area overlap between subject tree and its k^{th} competitor

A = area of subject tree's competition circle

and n = number of competitors

Figure 2. Geometric interpretation of Staebler's, Newnham's, and Gerrard's competition indices

EX = a constant to be determined

n = number of competitors

Bella also computed competition circle diameters as KC where C is the crown diameter of an open-grown tree of the same diameter as the stand tree under study and K is a constant adjustment factor.

Prediction equations relating CIO and d.b.h. to diameter increments of jack pine (Pinus banksiana L.), red pine (Pinus resinosa Ait), and several species of Eucalyptus yielded R^2 values ranging from .54 to .82.

Keister (1972) proposed exactly the same formula for individual tree competition as did Gerrard. The only difference between the two

that in most even-aged stands there is a relationship between stem diameter and total height, and the relationship is modified by stand density. He concluded that trees of the same age growing on similar sites should differ in their relationship of height and diameter according to differences in competition experienced by the trees in the past. To reflect these relationships, Keister computed competition radii as:

$$R = hc/2m$$

where R = competition radius of tree

h = total height

m = dead limb length (defined as length of bole without live branches)

c = crown radius predicted from the regression equation A + B (d.b.h.) for stand-grown trees

Thus, tall trees with wide crowns and short dead limb lengths will have longer competition radii than short trees with narrow crowns and large dead limb lengths.

In field trials Keister attempted to predict slash pine (Pinus elliottii Engelm.) diameter increments obtained from seven plantations. Coefficient of determination (R^2) values varied from .56 to .68 for the best prediction equations.

Another zone of influence model that has possible merit is Opie's zone count (Opie, 1968). It differs from other overlap models in that use is made of point sampling (Bitterlich, 1947; Grosenbaugh, 1958). Opie defines his measure of competition as

$$S = (BAF / \sum_{i=1}^{n} A_i) \cdot \sum_{i=1}^{n} (A_i \cdot i)$$

where S = basal area density (ft^2/acre) and the measure of competition

BAF = Basal area factor (ft^2/acre)

n = the largest number of circles, counting that of the subject tree, common to one point within the overlap zone

and A_i = the area covered by parts of i circles (counting that of the subject tree)

The competition radii in Opie's model are determined as PRF X DBH (PRF = plot radius factor) where PRF = (1/24) $\sqrt{(43{,}560-BAF)/BAF}$ (Dilworth and Bell, 1969). Once the PRF is determined, the components A_i, i and n are completely determined in Opie's model. Calibrating the model consists of finding the BAF which minimizes the mean square error in prediction equation relating S and other variables to the desired tree response.

The Point Density Concept

Other than Bitterlich's angle count technique of computing a point density in basal area per acre, Spurr's measure of point density has been the only one proposed. Spurr (1962) suggested that rather than choosing a fixed angle and making a one time estimate of basal area, a sequence of basal areas should be calculated at the point by letting the angle of view vary. The procedure is as follows:

1. A point is chosen.

2. Angles are chosen such that the basal area estimates are made on 1, 2, 3, ... to n tree samples.

3. Each of the basal areas of (2) are approximated by

$$B_k = (k - 1/2)\ 75.625\ \left(\frac{D_k}{L_k}\right)^2$$

where k = the number of trees in the sample

D_k = the d.b.h. of the tree exactly subtending the limiting angle

and L_k = the distance in feet of the tree from the point.

4. Spurr's point density is computed as

$$S_{pd} = \sum_{k=1}^{n} B_k/n$$

where S_{pd} = Spurr's point density

and n = the number of included trees where S_{pd} becomes approximately a constant.

Spurr claims that this procedure yields an estimate of basal area per acre which takes into consideration the sizes and spatial arrangement of the trees competing for the point. By choosing a

subject tree as a point, a measure of individual tree competition is the result. Spurr reported a correlation of .854 with Douglas-fir diameter increments.

Other Techniques

Other means of predicting basal area and diameter increments have been, with some success, to relate them to various measures of crown characteristics. Holsoe (1948), Arnold (1949), Ilvessale (1950), Monor (1951), Wile (1958), Warrack (1959), and Smith and Dubow (1960) all reported on the correlation of either basal area or diameter increments to one or more of the crown characteristics of width, length, volume, weight, and form. These relations, however, do not constitute competition models since they do not provide for any means of predicting the desired response over more than one period of time.

COMPETITION MODELING AND INVESTIGATIVE PROCEDURE

Extension of the Zone of Influence Concept

As previously noted, several writers have used the summation of weighted overlap areas as a measure of individual tree competition. Assuming this is a viable and biologically reasonable concept, an extension can be given.

In past modeling efforts, once the radii of influence for each tree in a unit had been determined and a subject tree chosen, all trees whose competition circles overlapped with the subject tree's were counted as competitors. For each competitor, its area of overlap with the subject tree was computed and taken as a measure of competitive stress between the subject tree and competitor. A function of the sum of the areas of overlaps was then formed to provide a measure of the total competitive stress exerted on the subject tree by its competitors. This procedure, however, implies that the subject tree and competitor compete equally for each point of growing space within their zone of overlap. Recognizing this as a possible inconsistency of past zone of influence modeling efforts, the following theoretical development is offered.

Consider the zone of influence of a tree that is centered at the origin of an x, y coordinate with competition radii, CR. The hypothesis that a subject tree and competitor do not compete equally for each point of growing space in their overlap zone suggests that

a tree does not have a uniform ability to compete throughout its zone of influence. That is, for a given point, x,y, in a tree's zone of influence, its ability to compete can be represented as $W(x,y,\underline{S})$, where $\underline{S}$ is a vector of tree characteristics such as height, crown width, and d.b.h. However, since the assumed shape of the zone of influence is circular, it is logical to assume that on circles of constant radii contained within the zone of influence a tree's ability to compete is constant on its circumference. Thus, $W(x,y, \underline{S})$ can be written as $W(R(x,y), \underline{S})$, where $R(x,y) = \sqrt{x^2 + y^2}$ and is the distance from the center of the competition circle to the point x,y. The function $W(R(x,y), \underline{S})$ will be called the tree's competitive force at x,y. Competitive force will be defined as the potential ability of a tree to compete in absence of competitors.

Now consider a subject tree (the i^{th}) centered at (x_i,y_i) and a competitor (the j^{th}) centered at (x_j,y_j). The competitive force functions of the subject tree and competitor can be written respectively as $W_i(R(x-x_i, y-y_i), \underline{S_i})$ and $W_j(R(x-x_j, y-y_j), \underline{S_j}$. $\underline{S_i}$ and $\underline{S_j}$ are, respectively, the tree characteristic vectors of the i^{th} and j^{th} tree. Shifting each tree's center to the origin was done so that the force functions proposed later could be written in terms of distance from tree center. These functions, however, define competitive forces when the trees are not in competition. That is, given a tree of known size and characteristics, it will be assumed that the force function represented above in abstract form will define that tree's potential ability to compete . When the competitive circles

of two trees overlap, they are assumed to be competing with each other, thus it might be visualized that at a point x_0,y_0 in the region of overlap, one tree's potential ability to compete is modified by the other. Since the objective is to define a measure of competitive stress exerted on a subject tree by a competitor the following function was defined as the competitive force exerted on the i^{th} subject by its j^{th} competitor. It is defined as:

$$CF_{ij}\ (x,y,\ \underline{S}_i,\ \underline{S}_j = RF_{ij}\ (x,y,\ \underline{S}_i,\ \underline{S}_j)W_j(R(x-x_j,\ y-y_j),\ \underline{S}_j)$$

where If $W_i(R(x-x_i,\ y-y_i),\ \underline{S}_i) > W_j(R(x-x_j,\ y-y_j),\ \underline{S}_j)$, then

$$RF_{ij}(x,y,\ \underline{S}_i,\ \underline{S}_j) = \frac{W_j(R(x-x_j,\ y-y_j),\ \underline{S}_j)}{W_i(R(x-x_i,\ y-y_i),\ \underline{S}_i)}$$

$$\text{If } W_i(R(x-x_i,\ y-y_i),\ \underline{S}_i) \leq W_j(R(x-x_j,\ y-y_j,\ \underline{S}_j) = 1$$

and where

1. $CF_{ij}\ (x,y,\ \underline{S}_i,\ \underline{S}_j)$ is the competitive force exerted on the i^{th} subject tree by its j^{th} competitor at the point (x,y)

and 2. $RF_{ij}\ (x,y,\ \underline{S}_i,\ \underline{S}_j)$ is a factor which reduces the competitive force of the j^{th} competitor at (x,y) if the competitive force of the subject tree is greater than that of the competition, but does not reduce it if the competitive force of the subject tree is less than that of the competitor. In other words, the competitive force exerted on the i^{th} subject tree by the j^{th} competitor, defined by the function $CF_{ij}(x,y,\ \underline{S}_i,\ \underline{S}_j)$, says:

1. Reduce the competitive force function of the j^{th} competitor by multiplying it by the ratio of competitive force function of the subject tree and competitor if the competitive force of the subject

tree is greater than the competitive force of the competitor.

2. Set the competitive force exerted on the i^{th} subject tree by the j^{th} competitor equal to the competitive force of the competitor, if the competitive force function of the subject tree is less than or equal to the competitive force of the competitor. That is, the competition force function of the competitor can be reduced but it can never be increased beyond its maximum value as defined by $W_j(R(x-x_j, y-y_j), \underline{S}_j)$.

3. The function defined by 1 and 2 is taken as the competitive force exerted on the i^{th} subject tree by its j^{th} competition at the point (x,y).

With an appropriate form for the competitive force function chosen, the total competitive stress exerted on the i^{th} subject tree by its j^{th} competitors can be defined by

$$S_{ij} = \int_{R_{ij}} CF_{ij}(x,y, \underline{S}_i, \underline{S}_j)dA$$

where $CF_{ij}(x,y, \underline{S}_i, \underline{S}_j)$ = the previously defined function

S_{ij} = the total competitive force exerted on the i^{th} subject tree by its j^{th} competitor

R_{ij} = the region of integration (the area overlap region between the i^{th} subject tree and its j^{th} competitor)

dA = Area differential = $d_x d_y$

If a tree has n competitors, then the total competitive force exerted on the i^{th} subject tree by its competitors, in the same vein as previous researchers, is given by

$$CF_i, ALL = \sum_{j=1}^{n} S_{ij}$$

where CF_i, ALL is the total competitive stress exerted on the i^{th} subject tree by all its competitors.

To finish the development, it is noted that the i^{th} subject tree's total competitive ability is

$$TCF_i = \int_{R_i} W(R(x-x_i, y-y_i), \underline{S}_i)dA$$

where TCF_i = the i^{th} subject tree's ability to compete

R_i = the region of integration and i^{th} subject tree's competition circle.

Conversely, the total ability of the i^{th} subject tree to compete, allowing for the competitive effects of its competitors, can be defined as $TAG_i = TCF_i - CF_i$, ALL. Now, suppose that two subject trees have the same value for CF_i, ALL, but one's TCF_i is larger than the other. If CF_i, ALL was taken as a measure of competition, both trees would be assigned the same competitive status even though the one with the larger TAG_i is in a better competitive position. To account for this situation, a logical procedure would be to subtract a constant times TAG_i from CF_i, ALL and define this quantity as the competition index. That is, the proposed competition index for the i^{th} subject tree is

1. $TAC_i = CF_i$, ALL - E (TAC_i)

or, upon rewriting

2. $TAC_i = E\ (\frac{1+E}{E}\ CF_i$, ALL - $TCF_i)$.

For the two data sets available, this approach to defining a competition index was compared with two existing models (Bella's and Gerrard's) in regard to their diameter increment prediction ability. It was hoped that, by defining the idea of competition on a point basis rather than a gross overlap basis, gains could be made.

Weight Function Choice

The only question that remains to be answered is what form should the weight function $W(x,y,\underline{S})$ have. One approach to deriving a possible form for $W(x,y,\underline{S})$ is to make the assumptions that

1. A tree exerts greater competitive force at the center of its competition circle and as one moves away from the center, competitive force continuously decreases.

2. A larger tree can exert more competitive force everywhere within its competition circle than a smaller tree can, and

3. On a circle of fixed radius, the competitive force is constant on its boundary.

With a tree of competitive radius (CR) centered at the origin, a function satisfying the above conditions is given by

$$W(x,y,\underline{S}) = M(\underline{S})[B_0 + B_1\ (R(x,y)/CR + B_2\ R^2(x,y)/CR^2]$$

where $M(\underline{S})$ is a function of tree size and when suitably chosen represents the maximum possible competitive force

and B_0, B_1, . . . are constants to be determined with the

$$\text{restrictions} \frac{dW(x,y,\underline{S})}{dR(x,y)} \leq 0,$$

and $$BO + B_1\ R(x,y)/CR + B_2\ R^2\ (x,y)/CR^2 \leq 1$$

Without previous knowledge as to what form $M(\underline{S})$ should take or how many terms should be included in the factor $B_0 + B_1\ R(x,y)/CR + B_2\ R(x,y)/CR^2 + \ldots$, nine trial forms were investigated. These were:

1. $B_0 + B_1\ R(x,y)/CR$

2. $CR^{EX}\ (B_0 + B_1\ R(x,y)/CR)$

3. $[S(HT\text{-}DL)CR^2]^{EX}\ [B_0 + B_1\ R(x,y)/CR]$

4. $B_0 + B_1 R(x,y)/CR + B_2 R^2(x,y)/CR^2$

5. $CR^{EX} (B_0 + B_1 R(x,y)/CR + B_2 R^2(x,y)/CR^2)$

6. $[S(HT-DL)CR^2]^{EX} (B_0 + B_1 R(x,y)/CR + B_2 R^2(x,y)/CR^2)$

7. 1

8. CR^{EX}

9. $[S(HT-DL)CR^2]^{EX}$

where HT = total tree height

DL = dead limb length

CR = competition radius

and EX, S, B_0, B_1, and B_2 are constants to be determined depending on the weight function form and data set.

Weight functions 7, 8, and 9 were the weight functions and the forms chosen for M($\underline{S}$). That is, these assumed functions provided a test of the hypothesis that a variable weight function was necessary. Among the weight functions 7, 8, and 9, 7 was a control which provided for the test of the hypothesis that M($\underline{S}$) was a function of tree size.

Determination of Weighted Areas of Overlap and Weighted Areas of Circles

When the weight function varied (contained the independent variables x and y) it was necessary to use numerical integration to evaluate the weighted areas of overlap. For these computations, a composite form of Simpson's Rule was used. Simpson's Rule is defined by:

$$I \simeq \frac{(b-a)}{b} [f(a) + 4 f[\frac{(b+a)}{2}] + f(b)] \quad \text{(Conte and de Boor, 1972)}$$

where $I \simeq$ approximate integral of $f(x)$, on $[a,b]$

$f(x)$ = the function to be integrated

a = lower limit of integration

b = upper limit of integration

Letting C_1 and C_2 be circles of radii R_1 and R_2 ($R_1 > R_2$) centered at respectively (0,0) and (0,D) in a X,Y coordinate system, the numerical integration procedure employed is:

1. The maximum value obtained by $y(y_{max})$ in the area of overlap is determined. y_{max} is calculated as

   a. $\sqrt{R_1^2 - z^2}$ if $D > R_1$, where $z = (R_1^2 - R_2^2 + D^2)/(2D)$, (the value of x where C_1 and C_2 intersect). The condition $D > R_1$ is the case where neither cirle overlaps the other circle's center.

   or b. R_2 if $D \leq R_1$ (the case where C_1 overlaps C_2's center).

2. The interval $[0, y_{max}]$ is partitioned as $[z_1, z_2, \ldots . z_7] = [0, 0 + E, 0 + 2E, \ldots\ldots, y_{max}]$ where $E = y_{max}/6$.

3. For each point in the partition in 2, the minimum value obtained by x, $(x(z_i)_{min})$ and the maximum value obtained by x $(x(z_1)_{max})$ in the overlap region on the intersecting line $y = z_i$ are determined. The value of $x(z_i)_{min}$ is

$$\sqrt{D - R_2^2 - z_i^2}$$

The value of $x(z_i)_{max}$ is

a. $\sqrt{R_1^2 - z_1^2}$ if $D > R_1 - R_2$ (the case where C_1 does not completely overlap C_2)

or b. $D + R_2$ if $D \leq R_1 - R_2$ (the case where C_1 completely overlaps C_2)

4. Each interval $[x(z_i)_{min}, x(z_i)_{max}]$ was partitioned as

$$[W_{1i}, W_{2i}, \ldots W_{7i}] = [x(z_i)_{min}, x(z_1)_{min} + 2E_i, \ldots, x(z_i)_{max}]$$

where

$E_i = (x(z_i)_{max} - x(z_i)_{min})/6$ and assuming $f(x,y)$ is the weight function, the approximate integrals I_i were computed for each $i = 1, 2, \ldots 7$, as

$$I_i = \frac{1}{6}\left[\frac{x(z_i)_{max} - x(z_i)_{min}}{2}\right]\left[(f(W_{1i})z_i) + 4f(W_{2i},z_i)\right.$$

$$+ f(W_{3_i},z_i)) + (f(W_{3_i},z_i) + 4f(W_{4i},z_i)$$

$$\left. + f(W_{5_i},z_i)) + (f(W_{5_i},z_i) + 4f(W_{6i},z_i) + f(W_{7i},z_i))\right] =$$

$$\left[\frac{x(z_i)_{max} - x(z_i)_{min}}{12}\right](f(W_{1i},z_i) + 2(f(W_{3i},z_i) + f(W_{5i},z_i))$$

$$+ 4[f(W_{4i},z_i) + f(W_{6i},z_i)] + f(W_{7i},z_i))$$

and

5. The approximated weighted area of overlap was then computed as

$$I = \frac{1}{6}\quad\frac{2y_{max}}{2}\quad(I_1 + 4I_2 + I_3) + (I_3 + 4I_4 + I_5) +$$

$$(I_5 + 4I_5 + I_7)$$

$$= \frac{y_{max}}{6}\quad[I_1 + 2(I_3 + I_5) + 4(I_2 + I4 + I_6) + I_7]$$

where y_{max} has been multiplied by 2 to account for other half of the area of overlap.

Fortunately, for the weight function forms examined in this study,

weighted areas could be obtained directly. The weighted area for weight function was

$$W_i(x,y,\underline{S}_i) = C(B_0 + B_1 R(x,y)/CR_i$$

$$\int_0^{CR_i} 2\pi C [B_0 + B_1 T/CR_i] TdT =$$

$$(\pi/e)C[3B_0 + 2B_1]CR_i^2.$$

For the form

$$W_i(x,y,\underline{S}_i) = C(B_0 + B_1 R(x,y)/CR_i + B_2 R^2(x,y)/CR_i^2$$

the weighted area was

$$\int_0^{CR_i} 2\pi C[B_0 + B_1 T/CR_i + B_2 T^2/CR_i^2] TdT =$$

$\frac{\pi C}{6} [6B_0 + 4B_1 + 3B_2] CR_i^2$, where C denotes any of the three constant weight functions forms previously described.

In the case where the weight functions did not depend on x or y, weighted areas of overlaps were evaluated by multiplying the simple area of overlap by the constant competitive force function formed from the constant weight functions and weighted areas were evaluated by multiplying the simple areas times the constant weight function.

An Extension to a Volume Overlap Model

In the zone of influence competition models, it is assumed that competition is expressible as a function of areas of overlaps between competition circles and areas of competition circles. These

models are two dimensional and do not directly take into consideration three dimensional tree characteristics such as height and dead limb length. Implicitly the models do consider height and dead limb length since height and dead limb length are correlated with competition radius. In order to take these relations into account, the component terms of model proposed in this study were replaced by their tree volume counterparts; that is a measure of competition may be defined by

$$TAC_i = CF_i,ALL-E(TCF_i - CF_i,ALL)$$

where

TAC_i = competition index for the i^{th} subject tree

CF_i,ALL = the sum of weighted volume overlaps between the i^{th} subject tree and its competitors

TCF_i = the weighted crown volume of the i^{th} subject tree

E = a constant to be determined

To provide a means of testing the proposed model, crown shape was assumed to be a cone and weight functions 7, 8, and 9 were used. No attempt was made to formulate a variable weight function since it became apparent while testing the weighted area overlap models that this would have been computationally infeasible.

Calculating Volume Overlaps

The proposed volume overlap model requires that one calculate the volume of overlap between two overlapping cones. The volume of a cone of height (h) and radius (R) is simply:

$$V = \pi/3\ hR^2$$

Calculating the volume of overlap between two cones of differing radii and height located in different regions of an x,y,z coordinate system, however, must be accomplished by numerical integration.

Letting 1) C_1 be a cone of radius R_1, tip height TH_1 and base height BH_1, with vertical axis perpendicular to the x,y plane and passing through (0,0,0) and 2) C_2 be a cone of radius R_2, tip height TH_2, and base height BH_2, with vertical axis perpendicular to the x,y plane and passing through (D,0,0), the following algorithm can be used to approximate the volume overlap between C_1 and C_2 (Figure 3).

1. If $BH_1 > BH_2$, assign the lower limit of integration (LL) the value BH_1; otherwise assign LL the value of BH_2. That is, no volume of overlap can occur in the region below LL.

2. Calculate the radius of each cone at the height LL as:

$$R_1' = TH_1 - (TH_1 - BH_1)LL/R_1$$

and

$$R_2' = TH_2 - (TH_2 - BH_2)LL/R_2$$

3. If $R_1' + R_2' \leq D$ the volume of overlap is zero; otherwise, go to 4 and continue.

4. Compute the upper limit of integration

$$UL = TH_1 - \frac{(TH_1 - BH_1)}{R_1} \quad [R_1(TH_2 - BH_2) +$$

$$R_2(TH_1 - BH_1)/R_1(D(TH_2 - BH_2) - R_2(TH_2 - TH_1)]$$

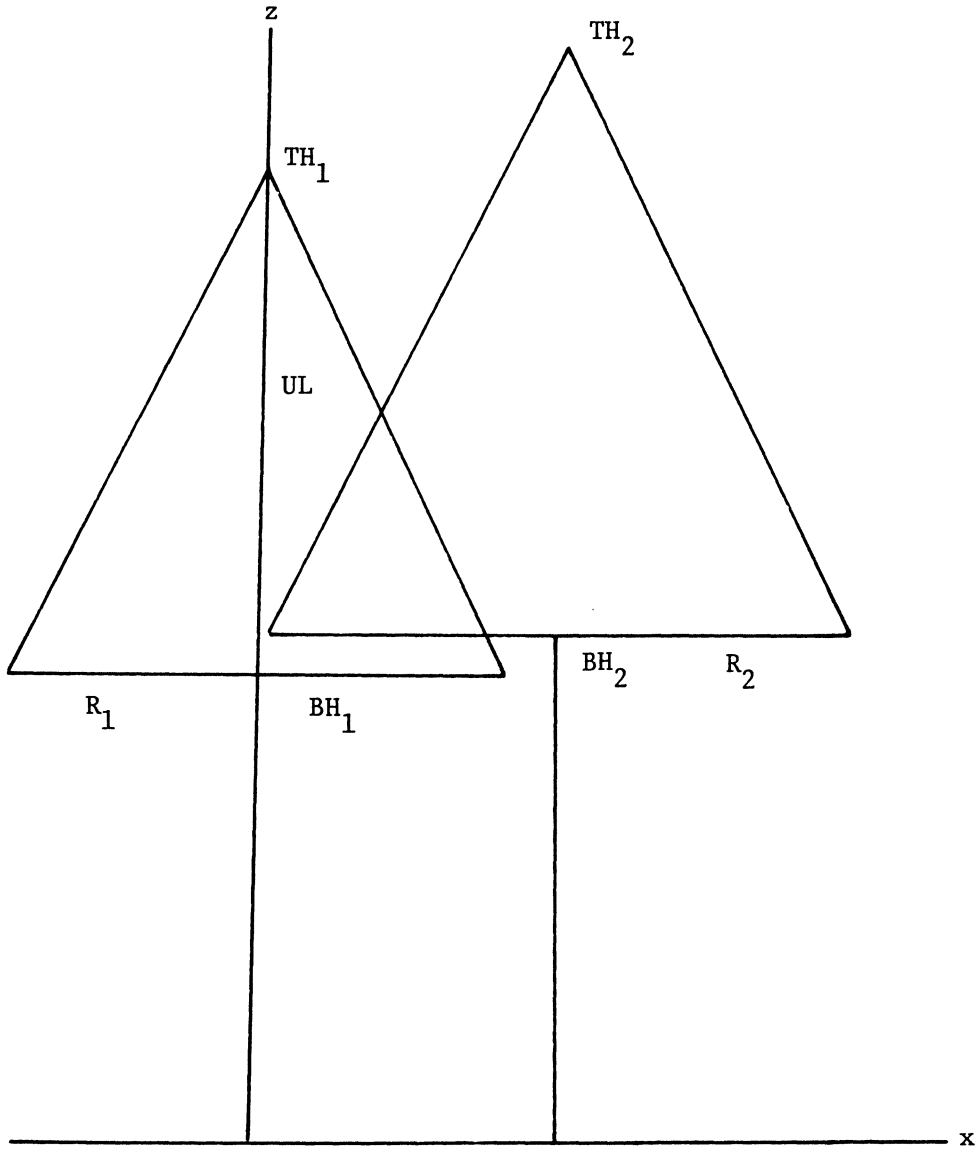

Figure 3. Projection of Two Overlapping Cones into the (x,z) Plane.

UL is the height along the Z axis where the two lines defined by

$$Z = TH_1 - \frac{(TH_1 - BH_1)X}{R_1}$$

and

$$Z = TH_2 - \frac{(TH_2 - BH_2)D}{R_2} \quad \frac{(TH_2 - BH_2)X}{R_2}$$

intersect (Figure 3).

5. Partition the interval (LL, UL) as $(W_1, W_2, \ldots, W_5)$ = (LL, LL + E, LL + 2E, . . . UL) where E = (UL-LL)/4.

6. For each partition point W_i, i = 1, 2, . . . 5

set $$R_{1i} = TH_1 - \frac{(TH_1 - BH_1)W_i}{R_1}$$

and $$R_{2i} = TH_2 - \frac{(TH_2 - BH_2)W_i}{R_2}$$. R_{1i} and R_{2i} are respectively the radii of C_1 and C_2 in the intersecting plane = W_i.

7. For each of the circle radii pairs (R_{1i}, R_{2i}) obtained in 6, compute the area of overlap with center to center distance (D). Call these areas A_i.

8. Approximate the volume overlap between C_1 and C_2 using Simpson's Rule by

$$V = \frac{(UL-LL)}{12} [(A_1 + 4A_2 + A_3) + (A_3 + 4A_4 + A_5)]$$

$$= \frac{UL-LL}{12} [A_1 + A_5 + 2A_3 + 4(A_2 + A_4)]$$

DATA COLLECTION AND COMPILATION

Data Collected

Data for testing and comparing the diameter increment prediction ability of selected existing and developed competition models were obtained from two Westvaco fertilizer study control plots. These plots are located near Appomattox, Virginia, and at the time of establishment by Westvaco in 1968, each plot was given an identification code,[1] and every tree within each plot numbered consecutively with aluminum tags beginning with the numeral "1". For reference purposes the plots will be referred to simply as plots 1 and 2.

Both are circular, one-tenth acre plots, located in old-field loblolly pine (Pinus taeda L.) plantations that were age 24 at the time of measurement in 1975. At the time of measurement, plots 1 and 2 had, respectively, 50 and 55 trees. Plot 1 contained 5 volunteer Virginia pine (Pinus virginiana mill.) trees, whereas plot 2 contained 6 Virginia pine wildlings. Site quality of each plot was average being, respectively, 55 and 50 feet at base age 25 years for plots 1 and 2.

From 1968 to 1972 each plot was visited yearly by Westvaco personnel and each living tree's d.b.h. recorded to the nearest tenth-inch.

---

[1]Plot 1 was Westvaco BaB-Reynolds Plot 101, and Plot 2 was Westvaco BaB-Reynolds Plot 217.

After 1972 the plots were not revisited until 1974, when Richard F. Daniels, a graduate student at Virginia Polytechnic Institute and State University, returned to each plot and recorded every tagged tree's rectangular coordinates with respect to an arbitrary origin. In 1975, the author returned to the plots and took from each living trees four increment cores. Beginning with the 1974 growth ring, yearly radial increments were measured to the nearest hundredth inch, extending back to the 1970 radial increment. The measurements were made with a measurement scale and vernier mounted on the table of a binocular scope. The average of the four radial increments for every measured year for each tree was taken as that tree's radial growth sequence for the years 1970 to 1974. Also, since the trees were bored to center, it was possible to measure the distance from the center to the end of the 1970 growth ring on each core. The average of 2 times these four distances for each tree provided an estimate of its d.b.h. (i.b.) at the beginning of the 1970 growth year.

For trees not living in 1975, radial increments were considerably harder to obtain. Fortunately, from mortality records, the author was able to piece together the dates of death of each tree not alive in 1975. These trees were sawed off at d.b.h. and cross sections removed from which the required measurements were taken.

By merging the data for living and dead trees it was possible to get a complete and accurate account of each tree's diameter growth pattern from 1970 to 1974. Other data collected at the 1975 visit were each tree's:

1. total height to the nearest one-half foot

2. dead limb length to the nearest one-half foot

3. average bark thickness at d.b.h. (the average of four measurements taken to the nearest 20th inch)

4. average d.b.h. (o.b.) as determined by the four tree caliper measurements

5. d.b.h. (o.b.) measured with a D-tape

6. four radial increments for each living tree (incomplete)

From 30 Virginia pines in the surrounding stands of Plots 1 and 2, the following measurements were obtained for each tree:

1. d.b.h. (o.b.) measured with a D-tape

2. average of four d.b.h.'s (o.b.) measured with a tree caliper.

3. average double bark thickness (the average of four measurements taken to the nearest 20th inch.

The mean heights of all trees in 1975 for Plots 1 and 2 were respectively 41.4 and 42.8 feet; and the respective mean d.b.h.'s taken by D-tape were 5.46 and 5.95 inches. These mean d.b.h.'s did not differ significantly at the .001 level, on each plot, from the respective mean average caliper d.b.h.'s of 5.51 and 6.01 inches. The test of hypotheses were made using a simple t-test given in Snedecor and Cochran (1960) for testing the significant differences between two means. In fact, pooling the data (dead trees not included) from Plots 1 and 2 and regressing d.b.h. (tape) on d.b.h. (caliper) yielded the regression curve

$$\text{d.b.h. (tape)} = .0001 + 1.0011 \text{ d.b.h. (caliper)}$$

$S_{y \cdot x} = .123, \quad R^2 = .991, \quad DF = 100$, where

$S_{y \cdot x}$ = the standard error of estimate, R^2 = proportion of variation about the mean d.b.h. (tape) accounted for by the regression on d.b.h. (caliper) and DF = degrees of freedom for the standard error of estimate. Test of the hypothesis that the intercept was zero and the slope was 1 could not be rejected at the .0001 probability level; thus, for all practical purposes, d.b.h. (tape) equals the d.b.h. calculated from the average of four caliper measurements. In other words, the tree cross sections were essentially circular.

For calibrating some of the proposed and tested individual tree competition models, it was necessary for each plot tree's total height and dead limb length to be known or closely approximated at the beginning of each year's measured diameter increment. Unfortunately, these data were not obtained except at the end of the 1975 season. Thus, for the years 1970 through 1974, it was necessary to predict these values. Since the plots had a small portion of volunteer Virginia pine trees, two different sets of prediction procedures needed to be developed -- one for predicting the total height and dead limb length of the loblolly pine trees and another for predicting the total heights and dead limb lengths of the Virginia Pine Trees.

Predicted Data

Prediction Procedures for Loblolly Pine

Data from a large yield study at VPI & SU (Burkhart *et al.*, 1972) were used to derive height and dead limb length prediction equations for old-field loblolly pines. The equations were:

1. $H_T = 3.228\ Hd^{.804}\ N^{.354/D}\ EXP\ [(3.228/A - 13.300/AD + 4.916/D]$

$S_{y \cdot x} = 2.866, \quad R^2 = .930, \quad DF = 365$

2. $DL = .077\ H_T^{1.526}\ N^{.343/D}\ D^{-12.285/A}\ EXP\ (27.466/a - 67.476/AD)$

$S_{y \cdot x} = 2.972, \quad R^2 = .912, \quad DF = 365$

where H_T = total tree height

H_d = average height of dominants and codominants

N = number of trees per acre

DL = dead limb length

D = d.b.h.

and A = stand age

The equations were based on data from 371 trees. The coefficients in equations 1 and 2 were estimated using a non-linear least square program written by the author. Equation 1 is of the form used by Burkhart and Strub (1974).

Equations 1 and 2 involved the independent variables H_d and D [d.b.h.(o.b.)], neither of which were known for any of the plots in any of the years preceding 1975. The previous d.b.h.'s for Plots 1 and 2 were predicted respectively by the equations:

3. d.b.h. = -.069 + 1.277 d.b.h. (i.b.)

$S_{y \cdot x} = .193, \quad R^2 = .986, \quad DF = 47$

and 4. d.b.h. = .331 + 1.176 d.b.h. (i.b.)

$S_{y \cdot x} = .182, \quad R^2 = .982, \quad DF = 39$

where d.b.h. = diameter breast high outside bark measured with a D-tape

Equation 3 was derived from the 49 loblolly pine d.b.h. (o.b.)

(D-tape), d.b.h. (i.b.) pairs measured in 1975 on Plot 1. Equation 4 was obtained from 42 similar observations from Plot 2. The data from both plots would have been pooled and a single equation developed except a statistical test that the two regressions were equal resulted in rejection at the .001 level (Searle, 1971). Apparently there were differences in bark growth between plots. The usual assumption of normality was made in the test. Hd's for each plot were predicted using

5. $H_d = SI \text{ EXP } [-13.440(1/A - 1/BA)]$

where A = stand age

SI = site index

and BA = base age = 25 years

Equation 5 was constructed using data from the same yield study as that used to compute equations 1 and 2.

The missing height and dead limb lengths for the years 1970 to 1974 for each plot tree were thus filled in by using Equations 1, 2, 3, 4, and 5. This was accomplished for each plot by

1. Adjusting the constant term of either equation 1 or 2, so that it exactly predicted a given tree's known 1975 height or dead limb length, whichever was appropriate. Values used in this step were the 1975 observations of known N, D, H_d and H_T.

2. Predicting the trees' heights and dead limb length for the years 1970 through 1974 by substituting N, H_d, A, and D for each year into equations 1 and 2. The value of H_d was obtained from equation 5, and the values of D were obtained from either equation 3 or 4,

depending on the plot.

3. Repeating 1 and 2 above for each loblolly pine in each plot.

Prediction Procedures for Virginia Pine

Unfortunately, no data set was available from which height and dead limb length prediction equations could be constructed for the volunteer Virginia pine trees. Due, however, to the small number and size (short) of the Virginia pine component, it was possible to obtain a crude estimate of previous dead limb lengths from the ground. On each tree the number of whorls was counted from ground line to the first live branch and an average rate of crown death was computed by dividing the 1975 dead limb lengths by the number of whorls counted. This average was subtracted from the 1975 dead limb length to yield the 1974 predicted dead limb length. Repeating this process produced the predicted 1974 through 1970 dead limb lengths. Although crude, this procedure probably was fairly accurate and, due to the small number of Virginia pine trees in each plot, it likely had little effect on future analyses of the data.

Heights for the Virginia pine component were needed in order to calibrate the volume overlap models. Since this component was minor, it was felt that any inaccuracies that would result if these heights were obtained from site index curves would be small. Graphically constructed Virginia Pine site index curves were available for the piedmont in Nelson, Clutter and Chaiken (1961) from which the required Virginia pine heights could be scaled, but to facilitate

computer processing, the graph in Nelson, Clutter and Chaiken (1961) was approximated using the simple monomolecular growth function (Lundgren and Dolid, 1970 and Grosenbaugh, 1965). Heights were scaled from the graph for 132 valies of site index and age arranged in a 12 x 11 factorial. The simple monomolecular growth function was fitted to the data by nonlinear least squares.

$$H = 1.127\ SI\ (1 - e^{-.054A})^{1.821}$$

$$Sy{\cdot}x = 1.843,\quad R^2 = .992,\quad DF = 129$$

where H = height in feet

SI = site index (base age = 50 years)

and A = total age

The site index levels were 40 through 90 feet in increments of 5 feet and the levels of age were 15 through 65 years in increments of 5 years.

To predict the heights for Virginia pines on the sample plots, a value of SI was chosen such that the fitted equation would exactly predict the known 1975 height. All preceding heights were predicted by substituting known tree age.

The regression "goodness of fit" statistics, Sy·x and R^2, for the Virginia pine height prediction equation have no statistical interpretation since it cannot be assumed that the scaled heights contain random error. In order to provide a statistically interpretable measure of the goodness of fit of the fitted model, the techniques of non-parametric statistics were used. An additional 120 heights were scaled from the graph at age, site index pairs drawn at random. For

each age, site index pair the absolute value of the difference between its scaled height and the height predicted for the fitted equation were computed. A P = .95 percent, 1 - α = .975 tolerance limit (Gibbons, 1972) was then placed on a maximum absolute difference between predicted and scaled height to provide a measure of the goodness of fit of the derived equation. The tolerance limit set is defined by

$$PR\ (P = .95 \text{ percent of the absolute differences} \leq 1.84 \text{ feet})$$
$$= 1 - \alpha = .975, \text{ where PR = probability of event}$$

Figure 4 shows the empirical distribution of the differences (not absolute differences) and its .95 percent confidence limits (Gibbons, 1972).

Other models fitted to the factorial data were the complex monomolecular model (Lundgren and Dolid, 1970) and the model proposed by Payandeh (1974). The models with estimated parameters were, respectively,

$$H_T = SI\ [(1.142 - 1.517\ EXP\ (-.044A)]$$
$$Sy \cdot x = 2.12,\quad R^2 = .989,\quad DF = 129$$

and

$$H_T = 1.310\ SI^{.927}\ [(1 - EXP\ (-.054A)]^{4.624\ SI^{-.235}}.$$
$$Sy \cdot x = 1.901,\quad R^2 = .992,\quad DF = 127$$

These models did not provide any better estimate than the simpler monomolecular form and were, thus, not used.

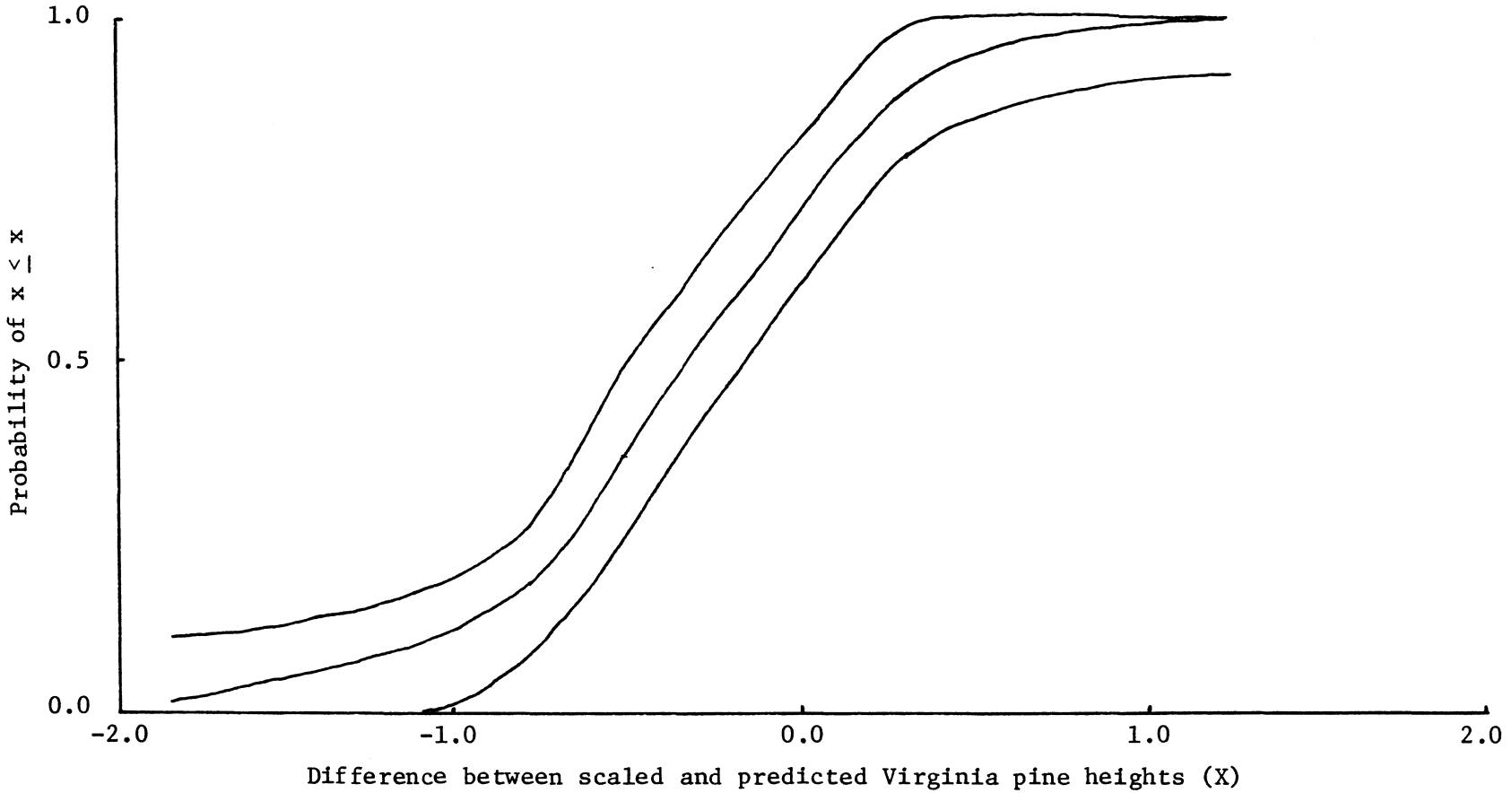

Figure 4. Empirical distribution function and 95 percent confidence limits for the difference between scaled and predicted Virginia pine height.

MODEL CALIBRATION

Data for Calibration

Since all of the proposed models and tested models were of the overlap type, the boundary trees from each plot could not qualify as subject trees. Consequently the trees on each plot were divided into interior and exterior trees. Interior trees were both subject trees and competitors, while exterior trees were exclusively competitors. Initially it was felt that for a tree to be classified as interior it should have at least two trees between itself and the plot boundary to eliminate boundary bias. Interior trees were thus chosen in this fashion. Exterior trees were then trees not classified as interior. The above scheme was borne out later because of the large calculated radii of some trees allowed these tree's competition circles to overlap with the competition circle of other trees beyond their immediate neighbors.

The exterior-interior classification scheme, however, drastically cut the number of subject trees in the already small plots. Plot 1 with 55 trees contained only 13 interior trees and Plot 2, with 50 trees, contained only 8 interior trees. This decrease in subject trees did not create an extreme problem in model calibration because the data set for both plots contained, for each tree, five years of yearly diameter increments. These five years of diameter increments thus provided, respectively, 65 and 40 observations for calibrating

models on the data in Plots 1 and 2. In other words, the objective was to calibrate the models using yearly observations instead of calibrating over a gross five-year period.

Parameter Estimation

For each of the previously listed individual tree competition models, from one to four model parameters had to be estimated in such a way that computed competition indexes were functionally related to corresponding diameter increments. Ideally, the function and estimated parameters chosen should be the ones which most closely predict diameter increments. Usually closeness of prediction is measured by either

$$(1) \ \max_{i=1,n} |A_i - P_i| \quad \text{or} \quad (2) \ \sum_{i=1}^{N} (A_i - P_i)^2/N$$

where A_i = measured value of i^{th} observation

P_i = predicted value of i^{th} observation

and N = number of observations.

Optimality is reached for either measure of closeness when the measure has been minimized over all functions and parameters. The measure $\sum_{i=1}^{N} (A_i - P_i)^2/N$ is the most familiar and the one which is almost always the easiest to handle mathematically and it will be used in this dissertation as the optimality criteria. Actually, the measure $\max_{i=1,n} |A_i - P_i|$ for the parameter estimation procedure presented in the next section poses no mathematical problems. In fact, by using the measure in programs written, computational time could have been reduced due to an enormous reduction in multiplication and squaring

operations. Future researchers might consider this as an optimality criteria.

Obviously it is impossible to entertain all possible functions in any estimation procedure; thus (1) a limited few likely functions, possibly based on experience would have to be chosen and the best selected from those limited few or (2) assume that the function has a Taylor's expansion

$$\sum_{i=1}^{\infty} \frac{f^{i}(0)x^{i}}{x^{1}}$$

and that the higher order terms sum to essentially zero. The latter course will be followed in this paper on the basis that it is objective and does not lead to a futile and unproductive search for the "best" functions. It is better to approximate a function than never find its true form.

From the above choice of prediction criteria and the assumption that the optimum function can be represented by the low order terms of a Taylor's expansion, the problem is to minimize for the calibrating data

$$S_k = \sum_{j=1}^{5} \sum_{i=1}^{N_k} [(I^k_{ij} - P^k L(CI^k_{ij})]^2, \quad k = 1, 2,$$

where

1. k equals plot number
2. j indexes the prediction year. j = 1, 2, 3, 4, 5,-- which is equivalent to 1970, 1971, 1972, 1973, 1974.
3. N_k equals number of interior trees in Plot k
4. i is the index of the i^{th} subject tree

5. I^k_{ij} is the diameter increment of the i^{th} subject tree in the j^{th} year on Plot k

6. CI^k_{ij} is the competition index of the i^{th} subject tree in the j^{th} year on Plot k

7. $P^i_L(\cdot)$ is a lower order polynomial of order L in CI^k_{ij} for Plot k

and 8. S_k = optimality criteria in Plot k.

In other words, for the data on each plot and model the procedure is to choose the model parameter and a low order polynomial which minimizes S_k.

Procedure of Parameter Estimation

Without any prior knowledge as to what degree of polynomial $P^k_L(C_{ij})$ was adequate to approximate the optimum functions $f^k(CI_{ij})$, k = 1, 2, it was necessary to calibrate each model for successively higher order polynomials until no higher order terms were statistically significant from zero. Tests were made at the .05 level and the customary assumption of normality and independence were evoked for the test. At this point in the investigation, no assumptions were made that the optimum function was invariant between plots or models. Later it was discovered any such assumption would have been unjustified for the models calibrated in this study. There were definite differences between plots in the degree of curvature exhibited between diameter increment and competition index as well as average slope.

The techniques of response surface were applied to the problem

of estimating the model parameters which minimized

$$S_k = \sum_{j=1}^{S} \sum_{i-1}^{N_k} [I^k_{ij} - P^k_L (CI^k_{ij})]^], \quad k = 1, 2$$

for each model of Tables 1 and 2.

The process of estimation employed a combination of the response surface methods of steepest descent, and canonical analysis. The technique of steepest descent is an optimum point seeking method used when an experimenter does not have a well conceived notion of the region in which the optimum point lies. Using this procedure an experimenter starts in a region, sometimes far from an optimum region, and sequentially moves along the path of steepest descent into a region close to or containing the sought optimum (Meyers, 1971). In the present study, steepest descent was used to move from an initial guess at the optimum model parameters to a better initial guess before further refinements were made by using a canonical analysis.

Once the experimenter is firmly convinced that no further gains can be made with the steepest descent method, a more detailed investigation of the response surface is made around the experimenter's best point. That is, once the steps of steepest descent have moved one into the approximate region where the optimum point lies, a detailed investigation is conducted in the region to locate the optimum point. One such technique for performing this investigation is known as canonical analysis (Meyers, 1971). Basically, canonical analysis consists of :

1. Designing an elaborate experiment in the suspected optimum region.

2. Fitting a second order response surface of the type:

$$Y = B_0 + \sum_{j=1}^{k} B_j X_j + \sum_{j=1}^{k} \sum_{m=1}^{k} B_{jm} X_j X_m + \sum_{j=1}^{k} B_{jj} X_j^2 \quad \text{where}$$

Y is the response, X_1, X_2 . . . X_k are independent variables related to Y and subscripted B's are regression coefficients.

3. Solving the fitted response surface for the point S_1^0, . . . S_k^0 of minimum predicted response, if one exists (the stationary point.)

and 4. Examining the fitted surface for a possible saddle point, falling ridge, or stationary ridge.

Letting $\underline{P} = \begin{bmatrix} P_1 \\ P_2 \\ \cdot \\ \cdot \\ \cdot \\ \cdot \\ P_{NP} \end{bmatrix}$

be a vector of NP model parameters and S the mean square error of prediction for any competition model, the algorithm of parameter estimation used in this study is

1. An initial guess $\underline{P}^0$ is made as to what the optimum should be. This guess should not be too far removed from the optimum region for otherwise computational time is increased.

2. Using $\underline{P}^0$ as a design center, a 2^{NP} factorial is formed in the parameters. Low levels are assigned the values $P^0_i - \varepsilon$, $i = 1, 2, \ldots NP$ and high levels are assigned the values $P^0_i + \varepsilon$

$i = 1, 2, \ldots NP$, where ε is a positive constant. Considerable experimentation with fitting models indicated a good choice for ε was .15.

3. S is evaluated for each of the design points in 2, including the design center, and the first order response surface $\hat{S} = \hat{B}_0 + \sum_{i=1}^{NP} \hat{B}_i P_i$ is fitted, where $\hat{S}$ is the estimated response, and the $\hat{B}_i$'s are the calculated regression coefficients.

4. The first point on the path of steepest descent is computed as

$$\underline{P}^1 = \underline{P}^0 + \frac{\varepsilon}{2\mu} \hat{\underline{B}} \quad \text{where } \hat{\underline{B}} = \begin{bmatrix} \hat{B}_1 \\ \hat{B}_{22} \\ \cdot \\ \cdot \\ \cdot \\ \hat{B}_{NP} \end{bmatrix}$$

and μ is a constant less than zero. A choice for μ that yielded fast convergence was $-\varepsilon/2$.

5. S is evaluated at $\underline{P}^1$ and is evaluated at the additional sequential points along the path of steepest descent defined by $\underline{P}^k = \underline{P}^0 + \frac{k\varepsilon}{2\mu} \hat{\underline{B}}$, $k = 2, \ldots$ until an evaluated S was greater than the one preceding it. In other words, adjusted estimates of the optimum point were made along the path until there was an actual increase in S.

6. $\underline{P}^0$ is set equal to the best estimate in 5 and steps 1 through 5 are repeated until a less than .5 percent decrease in S can be obtained.

7. Once the termination criteria for the steepest descent in 6 is met and the experimenter is satisfied that no additional gains can be made by repetition of 1 through 6, (1) a 3^{NP} factorial is designed about the last best estimate obtained in 6 and (2) a canonical analysis is performed as described in 8 through 18 below.

8. Letting P^{01} be the last best estimate from 6 and the design center for the 3^{NP} factorial described in 7, design levels were defined as:

a. low levels are assigned the values $P_i^{01} - \varepsilon$, $i = 1, 2, \ldots NP$

b. intermediary levels are assigned the values P_i^{01}, $i = 1, 2, \ldots NP$

c. high levels are assigned the values $P_i^{01} + \varepsilon$, $i = 1, 2, \ldots NP$.

9. The second order response surface

$$\hat{S} = \hat{B}_0 + \sum_{j=1}^{NP} \hat{B}_j P_j + \sum_{j=1}^{NP} \sum_{m=1}^{NP} \hat{B}_{jm} P_j P_m + \sum_{j=1}^{NP} \hat{B}_{jj} P_j^2$$

is fitted to the 3^{NP} design points in 8, where the single subscripted $\hat{B}_j$'s are calculated first order term regression coefficients and the double subscripted $\hat{B}_{jm}$'s are calculated second order term regression coefficients.

10. To make the second order response surface more amenable to analysis it is rewritten as:

$$\hat{S} = \hat{B}_0 + \underline{\hat{P}}'\underline{\hat{B}} + \underline{P}'\hat{B}\underline{P} \quad \text{where}$$

$\underline{P}'$ is the transpose of $\underline{P}$,

$$\underline{\hat{B}} = \begin{bmatrix} \hat{B}_1 \\ \hat{B}_2 \\ \cdot \\ \cdot \\ \cdot \\ \hat{B}_{NP} \end{bmatrix}$$

and

$$\underline{B} = \begin{bmatrix} \hat{B}_{11} & \hat{B}_{12/2} & \cdots & & B_{1NP/2} \\ & \hat{B}_{22} & B_{23/2} & \cdots & B_{2NP/2} \\ & & - & & \\ & & & - & \\ & & & & - \\ & \text{Symmetric} & & & \\ & & & & B_{NP,NP} \end{bmatrix}$$

11. Using the amended form of the response surface given in 10, the stationary point ($\underline{SP}^0$ of the response surface is computed as

$\underline{SP} = -\hat{B}^{-1}\underline{\hat{B}}/2$, where $\hat{B}^{-1}$ is the matrix inverse of $\hat{B}$.

12. The value of $\hat{S}$ at the stationary point is computed as $\hat{S}_0 = \hat{B}_1 + \underline{SP}^{0\prime}\underline{\hat{B}}/2$ where $\hat{S}_0 = \hat{S}$ evaluated at the stationary point and $\underline{SP}'$ = the matrix transpose of $\underline{SP}$.

13. The stationary point is translated to the origin by the linear transformation $\underline{Z} = \underline{P} - \underline{SP}$ and the response equation in 10 is rewritten as

$$\hat{S} = \hat{S}_0 + Z'\underline{BZ}$$

14. The additional transformation $\underline{Z} = M\underline{W}$ is formed where M is the NP x NP orthogonal matrix such that $M'\hat{B}M = \text{diag}\ (\lambda_1, \lambda_2, \ldots \lambda_{NP})$ where M' is the matrix transpose of M, diag denotes a diagonal matrix, and the λ_i's are the characteristic roots of $\hat{B}$.

15. Using the transformation in 13, the response surface of 12 is rewritten as:

$$\hat{S} = \hat{S}_0 + \underline{W}'\hat{M}'\hat{B}\hat{M}\underline{W} = \hat{S}_0 + \sum_{j=1}^{NP} \lambda_j W_j^2$$

16. If all the λ_i's are greater than zero, then any movement away from the stationary point will produce an increase in the response, and thus the estimated stationary point is a minimum point. When this condition was met, $\underline{P}^{01}$ was set equal to $\hat{SP}$ and steps 8 through 16 were repeated until less than a .1 percent decrease could be obtained in true response evaluated at the calculated stationary points. That is, for each stationary point obtained by repeating 8 through 16, if the decrease in actual response evaluated at the stationary point did not exceed .1 percent the algorithm is terminated.

17. If the λ_i's are mixed in sign then the stationary point is a saddle point. This condition was encountered only once and was handled as follows:

a. A new initial guess was made close to the stationary point

b. Steps 1 through 16 were repeated.

18. Once the algorithm is terminated, the last calculated stationary point is taken as the optimum point.

Although the algorithm above does not guarantee that the global minimum has been obtained, it does provide a means of estimating model parameters other than trial and error techniques. Although trial and error techniques probably yield reasonable estimates where the number of parameters is small (less than or equal to 3), as the number of parameters become larger the technique becomes an impossibility.

Thus, for all of the models calibrated in this study, the presented algorithm was used.

For a detailed account of the procedures used to formulate the above algorithm, the reader is referred to the works by Box and Wilson (1952) and Meyers (1971).

Determining Competition Radii, Heights and Dead Limb Lengths

Bella (1972) computed competition radii as K times the crown diameter of an open-grown tree of the same diameter as that of the stand tree. That is, competition radii were computed as $K\ CD = K(\hat{\alpha} + \hat{B}\ D)$ where CD = open grown crown diameter, D = diameter of stand tree, and $\hat{\alpha}$ and $\hat{B}$ are the regression coefficients from the regression of open-grown crown diameter on open-grown tree diameter. Gerrard (1969) simply set competition radii equal to K'D where D is the d.b.h. of the stand tree in question and K' is a scaling factor chosen such that it produced the largest R-square in regression models relating diameter increments to competition index. Gerrard's procedure was adopted for this study with the minor variation that instead of scaling diameter outside bark, competition radii were computed as K'd.b.h. (i.b.). Diameter inside bark were scaled to obtain competition radii because inside bark diameters were accurately known; scaling diameter outside bark values would have required that they be predicted.

Originally, it was felt that a species distinction should be made in computing competition radii. Models were calibrated

separately for loblolly and Virginia pine, and for the pooled data. Comparisons indicated that the separate species hypothesis did not decrease the mean square error for either plot over that of the mean square error obtained from not making the distinction. Either there is not any difference between the two species or the Virginia pine component was too small for any differences to be detected.

Trial calibrations were also made where competition radii were computed as $K(A + BD)$ where K = scaling factor, D = d.b.h. (i.b.) and A and B are constants to be determined by the model calibration procedure. Separate calibrations by species and calibrations with data combined for both species were made. Again, no increase in precision could be obtained over the simpler procedure of computing competition radii as KD with no species distinction made.

Calibrating the volume overlap models required that the two additional concepts of competition height and competition dead limb length be introduced. Mathematically, competition height was defined as S_1H_T and competition dead limb length was defined as S_2D_L where H_T and D_L are, respectively, a stand tree's total height and dead limb length, and S_1 and S_2 are constants and model parameters to be determined. These additional scaled dimensions have no interpretation like that of competition diameter but were needed for obtaining volume overlaps in the plots. Diameters at the base of the crown were assigned the value of the tree competition diameter (KD).

RESULTS AND DISCUSSION

Area Overlap Model

For the calibrating data of Plot 1, Table 1 shows: 1) the estimated optimum model parameters, 2) the coefficients of the polynomial regression equations relating diameter increments inside bark to competition index for the proposed competition model for each of the weight function forms. Table 2 presents the same results for the data of Plot 2.

All of the weight functions forms, except the ones involving the control form $W(\mathbf{X},Y,\underline{S}) = 1$, produced a model which accounted for approximately the same amount of variation in diameter increments within a plot. In Plot 1, R^2 ranged from .609 to .653 and in Plot 2, R^2 ranged from .826 to .830 depending on the weight function form. These results indicate that using a variable weight function form will probably not increase the precision of diameter increments predictions over those obtained by using a constant weight function form. Apparently, a tree competes with uniform force throughout its competition circle or the available data sets were not large enough to allow detection of any difference. In the writer's opinion, some gains may have been made by using a larger data base. Unfortunately, no larger data sets were available to test the hypotheses. Also, some of the failure to make improvements in predicting diameter increments by the use of a variable weight function may have resulted from

Table 1. Calibrations of Proposed Competition Models for Data from Plot 1

Weight Function Number	Weight Function[1] Form	Estimated Optimum Model[1] Parameters	R-Square (R^2), Mean Square Error (MSE), Calculated Polynomial Regression Coefficients (A_0 denotes the calculated intercept terms, A_1 and A_2 denote respectively the calculated first and second order terms). All regression coefficients are significant at the .05 level
1	$B_0 + B_1\ R(X,Y)/CR$	K=.922, E=-1.513, B_0=1.062, B_1 = .208	$A_0=.429\times10^{-1}$, $A_1=.340\times10^{-2}$, $A_2=-.131\times10^{-4}$, $MSE=.187\times10^{-2}$, $R^2=.619$
2	$CR^{EX}(B_0+B_1\ R(X,Y)/CR)$	K=.767, E=-1.531, EX=.345, B_0=.930, B_1=0.065	$A_0=.388\times10^{-1}$, $A_1=.484\times10^{-2}$, $A_2=-.267\times10^{-4}$, $MSE=.172\times10^{-2}$, $R^2=.650$
3	$[S(HT-DL)CR^2]^{EX}\cdot$ $(B_0+B_1R(X,Y)/CR)$	K=.467, E=-1.782, EX=-.235, S=1.536, B_0=.918, B_1=.251	$A_0=.366\times10^{-1}$, $A_1=.316\times10^{-1}$, $A_2=-.876\times10^{-3}$, $MSE=.178\times10^{-2}$, $R^2=.638$
4	$B_0 + B_1\ R(X,Y)/CR +$ $B_2\ R^2(X,Y)/CR^2$	K=.915, E=-.284, B_0=.832 B_1=.275, B_2=-.024	$A_0=.422\times10^{-1}$, $A_1=.425\times10^{-2}$, $A_2=-.205\times10^{-4}$, $MSE=.186\times10^{-2}$, $R^2=.619$
5	$CR^{EX}(B_0\ X\ B_1\ R(X,Y)/CR +$ $B_2\ R^2(X,Y)/CR^2)$	K=.723, E=-1.613, EX=.322, B_0=.805, B_1=.067, B_2=.052	$A_0=.393\times10^{-1}$, $A_1=.507\times10^{-2}$, $A_2=-.294\times10^{-4}$, $MSE=.178\times10^{-2}$, $R^2=.653$

Table 1--Continued

Weight Function Number	Weight Function Form	Estimated Optimum Model Parameters	R-Square (R^2), Mean Square Error (MSE), Calculated Polynomial Regression Coefficients (A_0 denotes the calculated intercept terms, A_1 and A_2 denote respectively the calculated first and second order terms). All regression coefficients are significant at the .05 level
6	$[S(HT-DL)CR^2]^{EX}(BO+B_1, R(X,Y)/CR + B_2R^2(X,Y)/CR^2$	K=.314, E=-1.984, EX=-.184, S=1.532, B_0=.873, B_1=.149, B_2=.135	$A_0=.363x10^{-1}$, $A_1=.473x10^{-1}$, $A_2=.217x10^{-2}$, MSE=$.177x10^{-2}$, R^2=.638
7	1	K=.927, E=-1.458	$A_0=.430x10^{-1}$, $A_1=.418x10^{-2}$, $A_2=0.199x10^{-4}$, MSE=$.192x10^{-2}$, R^2=.609
8	CR^{EX}	K=.748, E=-1.476, EX=.268	$A_0=.396x10^{-1}$, $A_1=.467x10^{-2}$, $A_2=-.251x10^{-4}$, MSE=$.175x10^{-2}$, R^2=.643
9	$[S(HT-DL)CR^2]^{EX}$	K=.365, E=-1.715, EX=-.220, S=.923	$A_0=.372x10^{-1}$, $A_1=.470x10^{-1}$, $A_2=-.195x10^{-2}$, MSE=$.179x10^{-2}$, R^2=.636

Table 2. Calibrations of Proposed Competition Models for Data from Plot 2

Weight Function Number	Weight Function Form	Estimated Optimum Model Parameters	R-Square (R^2), Mean Square Error (MSE), Calculated Polynomial Regression Coefficients (A_0 denotes the calculated intercept terms, A_1 and A_2 denote respectively the calculated first and second order terms). All regression coefficients are significant at the .05 level
1	$B_0 + B_1\ R(X,Y)/CR$	K=1.003, E=-.894, B_0=1.003, B_1=.095	$A_0=.222\times10^{0}$, $A_1=-.823\times10^{-3}$, $A_2=.911\times10^{-6}$, MSE=$.419\times10^{-3}$, R^2=.829
2	$CR^{EX}(B_0+B_1\ R(X,Y)/CR)$	K=1.005, E=-.976, EX=.117 B_0=1.025, B_1=-.084	$A_0=.227\times10^{0}$, $A_1=-.821\times10^{-3}$, $A_2=.875\times10^{-6}$, MSE=$.428\times10^{-3}$, R^2=.829
3	$[S(H_T-DL)CR^2]^{EX}$ · $(B_0+B_1\ R(X,Y)/CR)$	K=1.036, E=-.958, EX=.021, S=1.022, B_0=.927, B_1=.134	$A_0=.223\times10^{0}$, $A_1=-.690\times10^{-3}$, $A_2=.618\times10^{-6}$, MSE=$.426\times10^{-3}$, R^2=.826
4	$B_0+B_1\ R(X,Y)/CR + B_2\ R^2(X,Y)/CR^2$	K=1.032, E=-.932, B_0=.910, B_1=.052, B_2=-.083	$A_0=.226\times10^{0}$, $A_1=-.959\times10^{-3}$, $A_2=.117\times10^{-5}$, MSE=$.426\times10^{-3}$, R^2=.826
5	$CR^{EX}(B_0+B_1\ R(X,Y)/CR + B_2\ R^2(X,Y)/CR^2)$	K=1.014, E=-.939, EX=.111, B_0=.837, B_1=.044, B_2=-.066	$A_0=.229\times10^{0}$, $A_1=-.100\times10^{-2}$, $A_2=.127\times10^{-5}$, MSE=$.423\times10^{-3}$, R^2=.827

Table 2 --Continued

Weight Function Number	Weight Function Form	Estimated Optimum Model Parameters	R-Square (R^2), Mean Square Error (MSE), Calculated Polynomial Regression Coefficients (A_0 denotes the calculated intercept terms, A_1 and A_2 denote respectively the calculated first and second order terms). All regression coefficients are significant at the .05 level
6	$[S(HT-DL)CR^2]^{EX}(B_0+B_1\ R(X,Y)/CR + B_2\ R^2(X,Y)/CR^2)$	K=1.028, E=-.886, EX=.051, S=1.014, B_0=.918, B_1=-.034, B_2=-.167	$A_0=.226\times10^{0}$, $A_1=0.832\times10^{-3}$, $A_2=.894\times10^{-6}$, MSE=$.416\times10^{-3}$, R^2=.830
7	1	K=1.016, E=-.916	$A_0=.225\times10^{0}$, $A_1=0.910\times10^{-3}$, $A_2=.108\times10^{-5}$, MSE=$.434\times10^{-3}$, R^2=.827
8	CR^{EX}	K=1.014, E=-.990, EX=.271	$A_0=.229\times10^{0}$, $A_1=-.627\times10^{-3}$, $A_2=.473\times10^{-6}$, MSE=$.428\times10^{-3}$, R^2=.825
9	$[S(HT-DL)CR^2]^{EX}$	K=1.006, E=-.920, EX=.097, S=1.112	$A_0=.227\times10^{0}$, $A_1=-.568\times10^{-3}$, $A_2=.410\times10^{-5}$, MSE=$.422\times10^{-3}$, R^2=.827

inaccuracies in the numerical integrations. These inaccuracies could have been reduced by decreasing the partition interval length, but this would have increased the computer time necessary to calibrate a model from 30 minutes to over an hour on an IBM 370 executing FORTRAN G Level 21.

Although no differences appeared to exist between the choice of weight function form, excluding the weight function $W(X,Y,\underline{S}) = 1$, the dramatic difference between plots in the functional relation between diameter increments and TAC was not expected. The diameter increments of Plot 1 showed an increasing trend with increasing computed values of TAC regardless of the weight function, whereas the diameter increments of Plot 2 showed a decreasing trend with increasing TAC regardless of weight function. Figures 5 and 6 show, respectively, for Plots 1 and 2, graphs of diameter increment versus computed TAC, where TAC values were for the weight function form CR^{EX}. Similar graphs can be obtained for the other weight functions. The form CR^{EX} was chosen only for demonstration purposes.

The reverse in the trend between diameter increments and TAC would seem to indicate a failure of the proposed model, but close inspection of the model reveals that a trend reversal of this nature might be expected and that this reverse trend is most likely a function of stand age and diameter distribution. Actually the model did fail as a competition index since in one case it acted as a measure of competition while in another case it acted as a measure of growth. This failure, however, was also demonstrated by the two competition

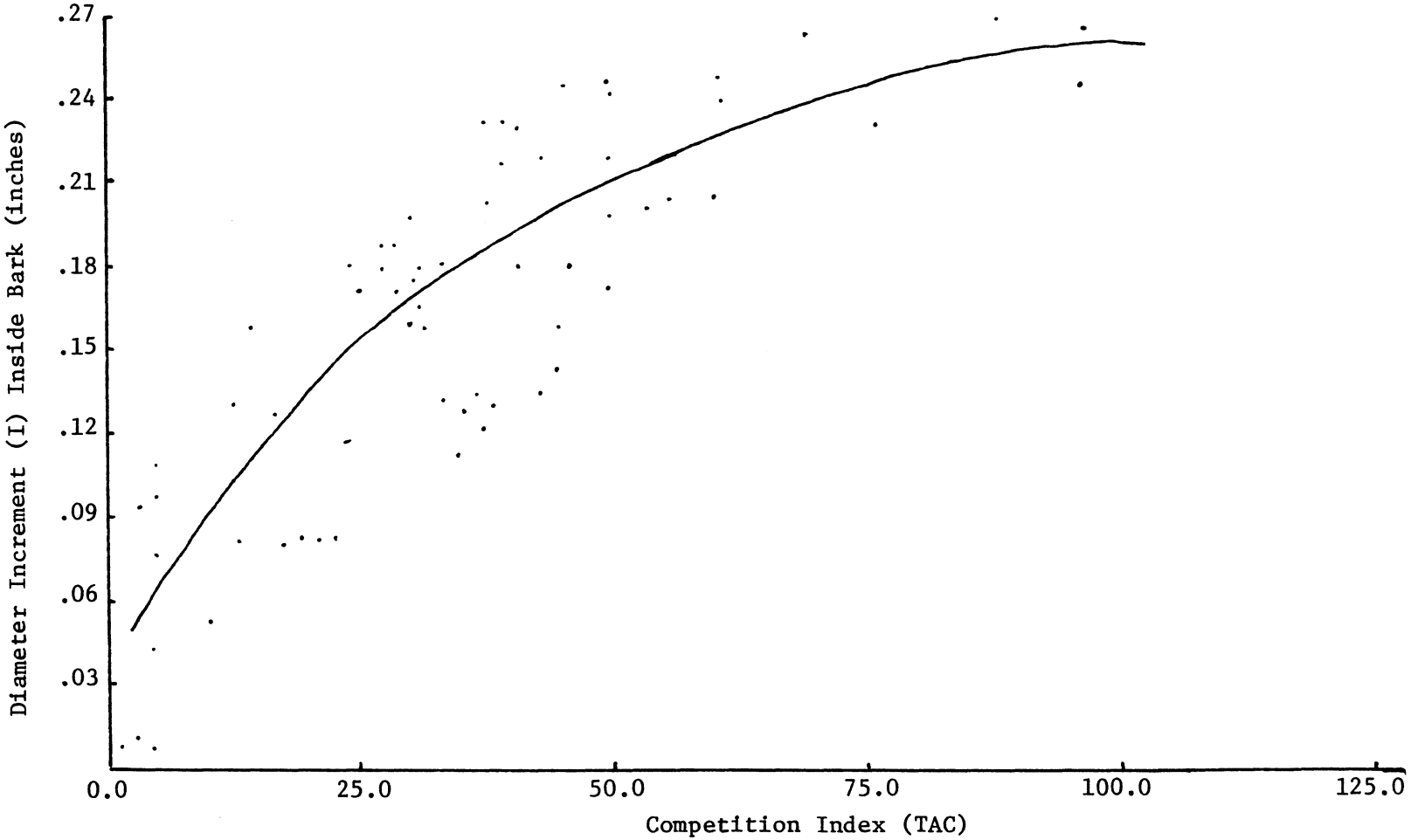

Figure 5. Scatter Diagram of diameter increment inside bark versus competition index, for Plot 1 Data, Proposed Area Overlap Model and Weight Function Form CR^{EX}

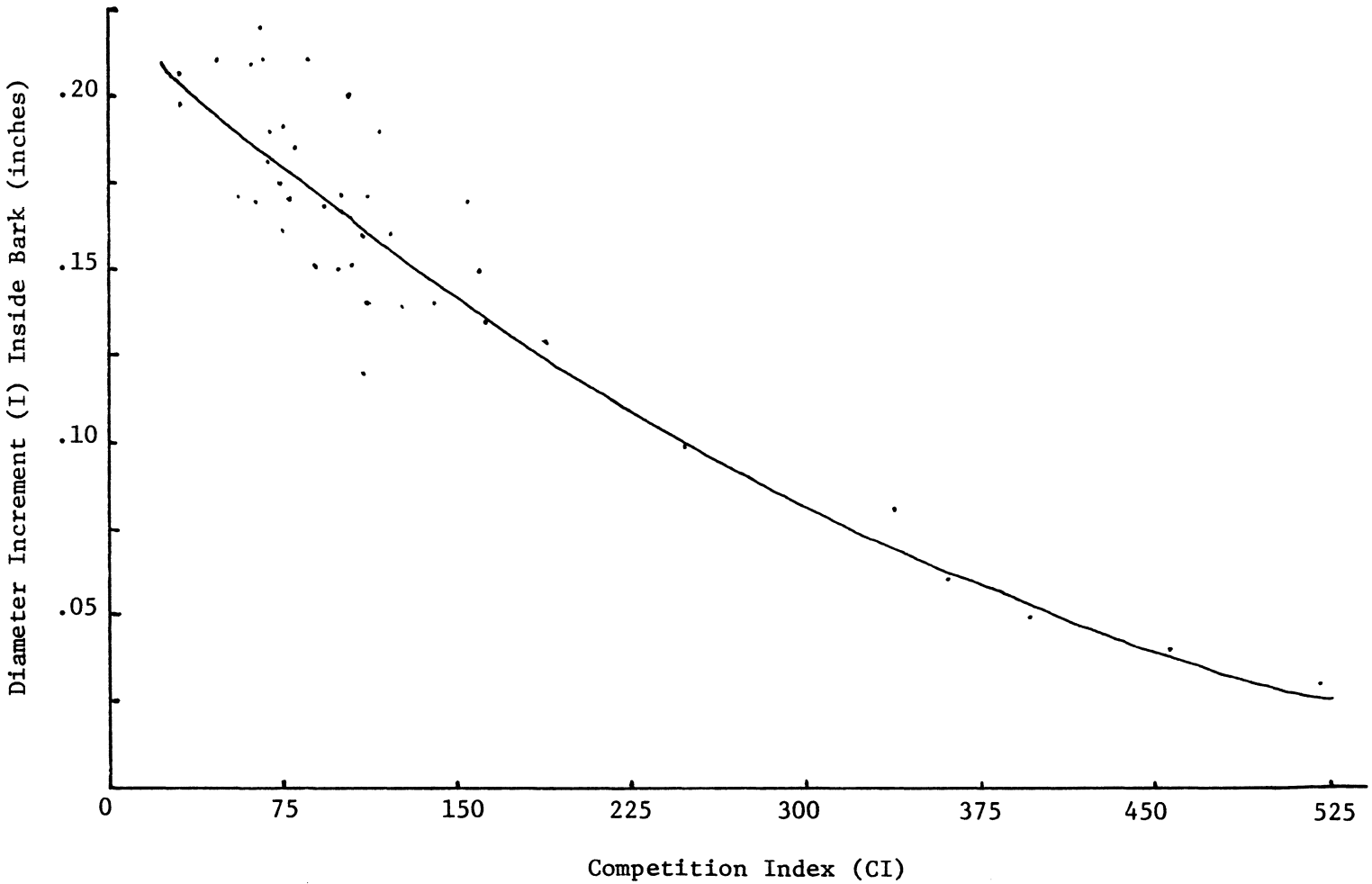

Figure 6. Scatter diagram of diameter increment inside bark versus competition index for Plot 2 data, proposed area overlap model, and weight function form CR^{EX}

models from the literature chosen for comparative purposes (see Tables 1 and 2).

The proposed model

$TAC_i = CF_i,ALL - E\ TAG_i$ can be written as

$$TAC_i = -E \quad \frac{(1+E)}{-E} \sum_{j=1}^{N} S_{ij} + TCG_i$$

and since all of the estimated optimum values of E were negative (see Tables 1 and 2), the model can be written as

$$TAC_i = E' \quad TCF_i + \frac{(1-E')}{-E} \sum_{j=1}^{N} S_{ij} \qquad \text{where}$$

$$E' = -E$$

Written in this form the model indicates:

1. If $E' < 1$, add $\frac{1-E'}{E'}$ times the sum of the weighted area overlap to the weighted area of the subject tree,

or 2. If $E' > 1$ subtract $\left|\frac{1-E'}{E'}\right|$ times the sum of the weighted area of the subject tree.

Regardless of the weight function form the estimated values of E' were greater than one for the Plot 1 data and less than one for Plot 2 data. Thus, in Plot 1, a constant times the sum of weighted area overlaps was subtracted from the weighted area of subject tree competition circles whereas, in Plot 2, they were added to the weighted areas of subject tree's competition circles. For illustrative purposes, the calibrated models for the data from Plots 1 and 2 and weight function form CR^{EX} were, respectively,

$$TAC_i = 1.476 \quad TCF_i - .322 \sum_{j=1}^{n} S_{ij} \quad , K = .748, EX = .268$$

and $$TAC_i = .990 \quad TCF_i + .010 \sum_{j=1}^{n} S_{ij} \quad , K = 1.014, EX = .271.$$

Comparing the diameter distributions of Plots 1 and 2, however, sheds some light on the nature of the expected trend of diameter increments and TAC_i and the role of E′. In Plot 1, diameters inside bark ranged from .96 inches to 5.45 inches over the five year calibrating period, with over 50 percent of the trees remaining below 3.5 inches d.b.h. (i.b.), while in Plot 2 diameters inside barks were evenly distributed in the range of 2.76 inches to 5.40 inches over the same period. Thus Plot 1 had a large number of small trees with relatively few larger trees while Plot 2 had a uniform diameter distribution in a small range. The nature of the diameter distribution in Plot 1 suggested that among small trees very few overlaps were occurring whereas more overlaps were occurring in the larger trees. That is, the ΣS_{ij} was greatest for larger trees and smallest for the small trees. As a result, when a tree was small, very little was subtracted from TCF_i, but as tree size increased, larger and larger amounts were subtracted from TCF_i. In other words, in Plot 1, TAC_i increased with increasing d.b.h. (i.b.) but the rate of increase became smaller as d.b.h. (i.b.) increased. Stated in another way, the second derivative of TAX_i with respect to d.b.h. (i.b.) is less than 0. Stated in still another way, the model reflects the fact that no matter how large a tree is in relation to its neighbors, it cannot grow any faster than its maximum potential rate.

For the Plot 2 data, the reverse situation is evident. Small trees are overlapped many times and

$$\sum_{j=1}^{n} S_{ij}$$

shows an increasing trend with decreasing d.b.h. (i.b.). Thus, the diameter increments tend to decrease with increasing TAC.

Possibly, depending on the diameter distribution, TAC can serve as a measure of individual tree advantage or disadvantage. However, within a given stand, diameter distribution changes over time; thus, the within stand role of TAC may change over time. That is, in a young stand TAC may serve as a measure of competitive disadvantage. This suggests that the model parameters change over time. Unfortunately, due to the limited number of yearly increments in the data sets, only a partial investigation of change in model parameters with time could be made. Time limitations of the study did not permit this investigation to be made on all the weight function forms, so changes over time for one weight function form were investigated. The weight function chosen was CR^{EX}. Each year's diameter increments were treated as a separate block of data. That is, the model calibration procedure was performed 5 times on each plot--one time for each year's increments--and the changes in model parameters were observed. Tables 3 and 4 show these results for Plots 1 and 2 respectively.

No trends could be detected in any of the parameters. This lack

Table 3. Change in Optimum Estimated Model Parameters Over Time for the Data Base of Plot 1, and Weight Function Form CR^{EX}, where CR = K d.b.h. (i.b.)

Stand Age	Model parameter			Polynomial regression coefficients. A_0 denotes the calculated intercept terms. A_1 and A_2 denote respectively the calculated coefficients of the first and second order term.			Mean square error of prediction	Percent of variation in diameter increment accounted for by regression
	K	EX	E	A_0	A_1	A_2		
19	.482	.334	-1.855	$.121 \times 10^{0}$	$.426 \times 10^{-2}$	-----	$.328 \times 10^{-3}$	74.9
20	.653	.295	-1.289	$.603 \times 10^{-1}$	$.538 \times 10^{-2}$	-----	$.564 \times 10^{-3}$	87.4
21	.506	.526	-1.732	$.524 \times 10^{-1}$	$.538 \times 10^{-2}$	-----	$.134 \times 10^{-2}$	74.3
22	.621	.764	-2.180	$-.673 \times 10^{-1}$	$.523 \times 10^{-2}$	$-.215 \times 10^{-4}$	$.917 \times 10^{-3}$	89.7
23	.722	.483	-1.596	$-.174 \times 10^{-1}$	$.415 \times 10^{-2}$	$-.162 \times 10^{-4}$	$.570 \times 10^{-3}$	92.8

Table 4. Change in Optimum Estimated Model Parameters Over Time for the Data Base of Plot 2, and Weight Function Form CR^{EX}, where CR = K d.b.h. (i.b.)

Stand Age	Model parameter			Polynomial regression coefficients. A_0 denotes the calculated intercept terms. A_1 and A_2 denote respectively the calculated coefficients of the first and second order term.			Mean square error of prediction	Percent of variation in diameter increment accounted for by regression
	K	EX	E	A_0	A_1	A_2		
19	1.104	.114	-1.264	$.243 \times 10^{0}$	$-.925 \times 10^{-3}$	$.127 \times 10^{-5}$	$.232 \times 10^{-3}$	89.8
20	1.043	.033	-.924	$.242 \times 10^{0}$	$-.554 \times 10^{-3}$	-----	$.143 \times 10^{-3}$	99.6
21	1.126	-.035	-.871	$.204 \times 10^{0}$	$-.447 \times 10^{-3}$	-----	$.264 \times 10^{-3}$	89.8
22	1.062	1.236	-1.201	$.182 \times 10^{0}$	$-.498 \times 10^{-3}$	-----	$.330 \times 10^{-4}$	98.2
23	.629	.982	-.519	$.183 \times 10^{0}$	$-.372 \times 10^{-3}$	-----	$.234 \times 10^{-3}$	92.4

of trend of estimated optimum parameter over time was the result of two factors operating. One was the small time interval and the other was the evidence of stationary ridges for the model parameters. Analysis of the fitted second order response surfaces (i.e., the response was mean square error and the independents were the model parameters), pointed to the conclusion that for each line in Tables 3 and 4 there existed many choices for the optimum estimated parameters. That is, there was a region such that little change in the mean square error would result for model parameters chosen from the region. These regions apparently intersected (one for each line in the tables) to result in the lack of trend of model parameters over time. One way of preventing this problem would have been to place restrictions on the solutions of the parameters. A possible restriction would have been to choose the optimum estimated parameters in each region such that it lies furthest away from all points in an adjacent region. Due to study time limitations, no attempt was made to impose the restriction or to isolate the regions of constant response.

To further evaluate the proposed area overlap model, two area overlap models were selected from the literature and calibrated for the data of each plot. The selected models were Gerrard's and Bella's. (See the "Background" section of this paper for definitions of these two models.) Competition radii were determined as K d.b.h. (i.b.) for Gerrard's model and as $C_0 + C_1$ d.b.h. (i.b.) for Bella's model. Actually, competition radii for Bella's model should have been calculated as some constant times the crown width of open-grown trees

with the same d.b.h. (o.b.). Open-grown data were not available and, as a result, the procedure above was adopted. Table 5 presents the results of these model calibrations for both plots. Neither model accounted for as much variation in diameter increment as did the proposed model. Both models accounted for about 78 percent of the variation in diameter increment for the Plot 2 data and compared favorably with the proposed model which accounted for approximately 83 percent of the variation in diameter increments. The percent of variation in diameter increments accounted for by Bella's and Gerrard's models for the Plot 1 data were, respectively, only 42.3 and 45.9 and were considerably less than those of the proposed model. Depending on the weight function, the proposed model, excluding the control weight function form $W(X,Y,S) = 1$, accounted for 63 to 66 percent of variation in diameter increments. Although neither comparison model accounted for as much variation in diameter increment as the proposed models, more important was the similar behavior of the trend of diameter increment and computed index for both the comparison model and the proposed model. Both comparison models showed an increasing trend with increasing diameter increment for Plot 1. The reverse trend was evident for both comparison models for Plot 2 data. These results imply that, as a class, the area overlap models may serve both as a measure of competitive advantage and as a measure of competitive disadvantage, depending on diameter distribution and stand age. Of course, it is always possible that Plot 1's data is an isolated occurrence with small probability of occurrence, but this is not likely

TABLE 5. Estimated Optimum Model Parameters, Polynomial Regression Coefficients, Mean Square Errors, and R-Square Values for the Comparison Models

Comparison Model	Plot Number	Estimated Optimum Model Parameters	R-Square (R^2), Mean Square Error (MSE), and Calculated Polynomial Regression Coefficients. B_0 denotes the calculated intercept terms, A_1 and A_2 denote respectively the calculated first and second order terms. All regression coefficients are significant at the .05 level
Gerrard's	1	K=1.478	$A_0=.783\times10^{-1}$, $A_1=.241\times10^{-3}$, $A_2=-.119\times10^{-6}$, $MSE=.280\times10^{-2}$, $R^2=.423$
Gerrard's	2	K=1.169	$A_0=.196\times10^{0}$, $A_1=-.425\times10^{-4}$ $MSE=.471\times10^{-3}$, $R^2=.772$
Bella's	1	$B_0=.018$, $B_1=1.360$, EX=-2.205	$A_0=.625\times10^{-1}$, $A_1=.355\times10^{-1}$ $A_2=-.233\times10^{-2}$, $MSE=.263\times10^{-2}$, $R^2=.459$
Bella's	2	$B_0=.021$, $B_1=1.057$, EX=-.666	$A_0=.178\times10^{0}$, $A_1=.946\times10^{-2}$, $A_2=-.271\times10^{-2}$, $MSE=.489\times10^{-3}$, $R^2=.769$

since in this case its probability of being selected for study would have been small. The writer believes that had previous researchers worked with younger stands, these trends would have been observed and probably quite frequently.

Volume Overlap Models

Tables 6 and 7 present, respectively, for the data bases of Plots 1 and 2, the calibration statistics for the extension to a volume overlap model. No gains were made by this approach but no loss of precision in predicting diameter increments was observed either. Had crown dimensions been more closely known, small gains probably would have been made. The model, however, does deserve further investigation. If it had been possible to specify crown shape more precisely, instead of assuming a cone, and had it not been necessary to predict heights and dead limb length, better estimates of diameter increments would have probably resulted.

TABLE 6. The Calibrated Volume Overlap Models for Plot 1 Data

Weight Function Number	Weight Function Form	Estimated Optimum Model Parameters	R-Square (R^2), Mean Square Error (MSE), Calculated Polynomial Regression Coefficients. A_0 denotes the calculated intercept terms, A_1 and A_2 denote respectively the calculated first and second order terms. All regression coefficients are significant at the .05 level.
7	1	K=.915, E=-1.482, S_1=1.298, S_2=.797	A_0=.609x10^{-1}, A_1=.303x10^{-3}, A_2=-.121x10^{-6}, MSE=.200x10^{-2}, R^2=.593
8	CR^{EX}	K=.371, E=-1.181, EX=-1.329, S_1=1.440, S_2=.568	A_0=.440x10^{-1}, A_1=.274x10^{-2}, A_2=-.854x10^{-5}, MSE=.166x10^{-1}, R^2=.662
9	$[S_1HT-S_2DL)CR^2]^{EX}$	K=.253, E=-1.612, EX=-.207, S_1=1.351, S_2=1.158	A_0=.553x10^{-1}, A_1=.628x10^{-2}, A_2=-.466x10^{-4}, MSE=.154x10^{-2}, R^2=.691

TABLE 7. The Calibrated Volume Overlap Models for Plot 2 Data

Weight Function Number	Weight Function Form	Estimated Optimum Model Parameters	R-Square (R^2), Mean Square Error (MSE), Calculated Polynomial Regression Coefficients. A_0 denotes the calculated intercept terms, A_1 and A_2 denote respectively the calculated first and second order terms. All regression coefficients are significant at the .05 level
7	1	K=.985, E=-.601,	A_0=.222x10^{0}, A_1=.175x10^{-3},
		S_1=1.482, S_2=.012	A_2=.395x10^{-7}, MSE=.462x10^{-3}, R^2=.822
8	CR_{EX}	K=1.043, E=-.227, EX=.146	A_0=.221x10^{0}, A_1=-.129x10^{-3},
		S_1=1.217, S_2=-.188	A_2=.212x10^{-7}, MSE=.434x10^{-3}, R^2=.823
9	$[(S_1HT-S_2DL)CR^2]^{EX}$	K=.799, E=-1.145, EX=0.448	A_0=.231x10^{0}, A_1=-.900x10^{-3},
		S_1=1.372, S_2=.564	A_2=-.865x10^{-5}, MSE=.455x10^{-3}, R^2=.814

LITERATURE CITED

Aaltonen, V. T. 1926. On the space arrangement of trees and root competition. Jour. Forestry 24: 627-644.

Arnold, D. L. 1949. Growing space ratio as related to form and development of lodgepole pine. Unpublished M.F. Thesis. Univ. British Columbia. 127 pp.

Bella, I. E. 1972. A new competition model for individual trees. Forest Sci. 17:364-374.

Bitterlich, W. 1947. Die Winkelzahlmessung. Allg. Forest U. Holzwirts. Ztg. 58: 94-96.

Box, G. E. P. and K. B. Wilson. 1952. On the experimental attainment of optimum conditions. J. Roy. Statist. Soc. B. 13.2.

Brown, A. S. 1965. Point density in stems per acre. New Zeal. For. Research Note 38. 11 pp.

Burkhart, H. E. and M. R. Strub. 1974. A model for simulation of planted loblolly pine stands. Growth models for tree and stand simulation. International Union of Forestry research organizations working party S4. 02-4. Proceedings of meeting in 1973. Royal College of Forestry, Stockholm, Sweden. pp. 128-135.

Burkhart, H. E., R. C. Parker, M. R. Strub, and R. G. Oderwald. 1972. Yields for old-field loblolly plantations. Division of Forestry and Wildlife Resources. Virginia Polytechnic Institute and State University, Publication FWS-3-72. 51 pp.

Conover, W. J. 1972. Practical nonparametric statistics. John Wiley and Sons, Inc., New York. 462 pp.

Conte, S. D. and C. DeBoor. 1972. Elementary numerical analysis: an algorithmic approach. McGraw-Hill Book Company, New York. 396 pp.

Dawkins, H. C. 1960. The Sudden Clinal Plot: thinning experiments without surrounds. Empire Forestry Rev. 39, pp. 168-172.

Dilworth, J. R. and J. F. Bell. 1969. Variable plot cruising. O.S.U. Book Stores, Inc., Corvallis, Oregon, 127 pp.

Gerrard, D. J. 1969. Competition quotient: A new measure of the competition affecting individual forest trees. Mich. State Univ., Agr. Exp. Sta., Research Bulletin 20. 32 pp.

Gibbons, J. D. 1972. Non-parametric statistical reference. McGraw-Hill Book Company. New York, N.Y. 306 pp.

Grosenbaugh, L. R. 1958. Point sampling and line sampling: Probability theory, geometric implications, synthesis. Southern For. Exp. Sta. Occas. Paper. 160. 34 pp.

Grosenbaugh, L. R. 1965. Generalization and reparametrization of some sigmoid and other non-linear functions. Biometrics 21: 708-714.

Gruschow, G. F. and T. C. Evans. 1959. The relation of cubic-foot volume growth to stand density in young slash pine stands. Forest Sci. 5: 59-65.

Holsoe, T. 1948. Crown development and basal area growth of red oak and white ash. Harvard Forest papers.

Ilvessale, Y. 1950. On the correlation between crown diameters and the stems of trees. Comm. Inst. For. Fenn 38 (pp. 1-32 in reprint).

Johnston, D. R. and W. T. Waters. 1962. Thinning control. Jour. Forestry 52. 65-74.

Keister, T. D. 1972. A measure of the intraspecific competition experienced by an individual tree in a planted stand. La. State Univ., Agr. Exp. Sta., Bull. No. 652. 23 pp.

Krajicek, J. E. and K. A. Brinkman. 1957. Crown development: An index of stand density. USDA Forest Service Central States Exp. Sta., Note 108. 3 pp.

Lundgren, A. L. and W. A. Dolid, 1970. Biological growth functions describe published site index curves for lake states timber species. USDA Forest Serv. North Central Forest Exp. Sta. Res. Pap. NE-36. 9 pp.

Meyers, R. H. 1971. Response surface methodology. Allyn and Bacon, Inc., Boston. 246 pp.

Minor, C. O. 1951. Stem-crown diameter relations in southern pine. Jour. Forestry 49: 490-493.

Moore, J. A., C. A. Budelsky and R. C. Schlesinger. 1973. A new index representing individual tree competitive status. Can. Jour. Forestry Research 3: 495-500.

Nelson, T. C., J. L. Clutter and R. C. Chaiken. 1961. Yield of Virginia Pine. USDA Forest Service, Southeastern Forest Experiment Station. Sta. Paper No. 124. 11 pp.

Newnham, R. M. 1964. The development of a stand model for Douglas-fir. Unpublished Ph.D. Dissertation, Univ. B.C. 202 pp.

Opie, J. E. 1968. Predictability of individual tree growth using various definitions of competing basal area. Forest Sci. 14 314-323.

Osborne, J. G. 1939. A design for experiments in thinning forest stands. Jour. Forestry 37: 296-304.

Payandeh, B. 1974. Formulated site index curves for major timber species in Ontario. Forest Sci. 20: 143-144.

Rogers, S. W. 1935. Soil factors in relation to root growth. Trans. 3rd. Inter. Cong. Soil Sci. I: 249-253.

Searle, S. R. 1971. Linear models. John Wiley and Sons, Inc. New York, New York. 532 pp.

Smith, H. F. and D. A. Dubow. 1960. Crown length and crown ratio as indicators of diameter growth in loblolly pine. Forest Sci. 6: 164-168.

Smith, J. Harry G. 1959. Comprehensive and economical designs for studies of spacing and thinning. Forest Sci. 5: 237-245.

Smith, J. Harry G. 1964. Root spread can be estimated from crown width of Douglas-fir, lodgepole pine and other British Columbia tree species. Forestry Chron. 40: 456-473.

Snedecor, George W. and W. G. Cochran. 1967. Statistical methods. Sixth edition. The Iowa State University Press, Ames, Iowa. 593 pp.

Spurr, S. H. 1962. A measure of point density. Forest Sci. 8: 85-95.

Staebler, G. R. 1951. Growth and spacing in an even-aged stand of Douglas-fir. Unpublished MF. Thesis, University of Michigan.

Vezina, P. E. 1962. Crown width--d.b.h. Relationships for open grown trees. For. Chron. 38: 463-473.

Warrack, G. C. 1959. Crown diameter, initial diameter and diameter growth in a young stand of Douglas-fir. Forestry Chron. 35: 150-155.

Wicht, C. L. 1936. Thinning research techniques. USDA Forest Service, Trans. 224. 61 pp.

Wile, B. C. 1958. A preliminary study of current diameter and height growth of spruce fir as influenced by crown volume, weight, and form, and by competition of surrounding trees. Dominion For. Serv., Ottawa, Canada. Bull. No. 1560.

Wilson, F. G. 1955. Evaluation of three thinnings at Star Lake. Forest Sci. 1: 227-232.

The vita has been removed from the scanned document

AN INVESTIGATION, COMPARISON, AND DEVELOPMENT OF INDIVIDUAL TREE COMPETITION MODELS

by

Thomas G. Matney

(ABSTRACT)

A new individual tree competition model based on the zone of influence principle was developed and tested on data from two young loblolly pine plantation stands. Analyses indicated that, depending on stand, diameter distribution and spatial arrangement, the model acted either as a competition advantage or as a competition disadvantage model. Attempts to discover the nature of the change in behavior of the model within stands over time were made by considering model parameters as functions of time and observing their change. The attempt was unsuccessful due to the limited number of years for which data were available. Comparisons of the developed model with two zone of influence models selected from the literature verified that at, least for the data used in this study, the selected comparison models could also serve as either a competitive advantage or disadvantage model, depending upon stand conditions. Also, neither comparison model predicted diameter increments with the same degree of precision as did the developed model.

An additional effort was made to define an individual tree competition model based on volume overlaps between the crowns.